Final Report

Project Title **Theoretical investigation of excited-state intermolecular proton transfer in 1*H*-pyrrolo[3,2-*h*]quinoline (PQ) with methanol and water clusters and intramolecular proton transfer in 2-(iminomethyl) phenol derivatives**

By **Nawee Kungwan**

June/ 2013 (14)

Contract No. MRG5480294

Final Report

Project Title Theoretical investigation of excited-state intermolecular proton transfer in 1*H*-pyrrolo[3,2-*h*]quinoline (PQ) with methanol and water clusters and intramolecular proton transfer in 2-(iminomethyl) phenol derivatives

Researcher Institute

Dr. Nawee Kungwan Chiang Mai University

Prof. Dr. Supa Hannongbua Kasetsart University

Dr. Mario Barbatti Max-Planck-Institut fuer kohlenforschung

This project granted by the Thailand Research Fund

Abstract

Project Code : MRG5480294

Project Title : Theoretical investigation of excited-state intermolecular proton transfer in 1H-pyrrolo[3,2-h]quinoline (PQ) with methanol and water clusters and intramolecular proton transfer in 2-(iminomethyl) phenol derivatives

Investigator : Dr. Nawee Kungwan

E-mail Address : naweekung@hotmail.com, naweekung@gmail.com

Project Period : 2 years (1st July 2011 to 30th June 2013)

Abstract:

The dynamics of ultrafast excited-state multiple intermolecular proton transfer (PT) reactions in complexes of 1*H*-pyrrolo[3,2-*h*]quinoline with water and methanol ($PQ(H_2O)_n$ and $PQ(MeOH)_n$, where n = 1, 2) is modeled using quantum-chemical simulations. The minimum energy ground-state structures of the complexes are determined. Molecular dynamics simulations in the first excited state are employed to determine reaction mechanisms and the time evolution of the PT processes. Excited-state dynamics results for all complexes reveal synchronous excited-state multiple proton transfer (ESmultiPT) via solvent-assisted mechanisms along an intermolecular hydrogen-bonded network. In particular, excited-state double proton transfer (ESDPT) is the most effective, occurring with the highest probability in the PQ(MeOH) cluster. The PT character of the reactions is suggested by nonexistence of crossings between $\pi\pi^*$and $\pi\sigma^*$ states.

Keywords: Excited-state proton transfer (ESPT), solvent assisted proton transfer, 1*H*-pyrrolo[3,2-h]quinoline, RI-ADC(2) dynamics simulations

Final report content:

1. Abstract

In Thai:

ไดนามิกส์ของการถ่ายโอนโปรตอนระหว่างโมเลกุลในสภานะกระตุ้นของ 1-เฮชไพโร[3,2-*h*]ควิโนลิน (พีคิว) กับโมเลกุลของน้ำและเมทานอลถูกศึกษาโดยวิธีจำลองทางเคมีควอนตัม พลังงานต่ำสุดของโครงสร้างในสภานะพื้นได้ถูกทำนายก่อน จากนั้นการจำลองทางเมโมกุลไดนามิกส์ในสภาวะกระตุ้นที่หนึ่งถูกใช้ในการหากลไกลปฏิกิริยาและเวลาในการเกิดการถ่ายโอนโปรตอน ผลจากการจำลองทางไดนามิกส์ได้พบว่าปฏิกิริยาการถ่ายโอนโปรตอนของทั้งสี่ระบบที่ทำการศึกษาเป็นการถ่ายโอนโปรตอนแบบหลายโปรตอนในเวลาใกล้เคียงกันโดยการถ่ายโอนโปรตอนนั้นถูกทำให้เร็วขึ้นด้วยโมเลกุลของสารละลายซึ่งคือน้ำและเมทานอลที่เข้ามาสร้างเครือข่ายพันธะไฮโดรเจน โดยเฉพาะปฏิกิริยาการถ่ายโอนโปรตอนแบบสองตัวในเวลาเดียวกันของสารพีคิวกับเมทานอลให้ความน่าจะเป็นในการถ่ายโอนโปรตอนสูงสุด ทั้งนี้คุณลักษณะของการถ่ายโอนโปรตอนถูกยืนยันด้วยพลังงานที่ไม่ซ้อนทับกันระหว่างชั้นพลังงาน ไพ-ไพสตาร์ และ ไพ-ซิกมาสตาร์

In English:

The dynamics of ultrafast excited-state multiple intermolecular proton transfer (PT) reactions in complexes of 1*H*-pyrrolo[3,2-*h*]quinoline with water and methanol ($PQ(H_2O)_n$ and $PQ(MeOH)_n$, where n = 1, 2) is modeled using quantum-chemical simulations. The minimum energy ground-state structures of the complexes are determined. Molecular dynamics simulations in the first excited state are employed to determine reaction mechanisms and the time evolution of the PT processes. Excited-state dynamics results for all complexes reveal synchronous excited-state multiple proton transfer (ESmultiPT) via solvent-assisted mechanisms along an intermolecular hydrogen-bonded network. In particular, excited-state double proton transfer (ESDPT) is the most effective, occurring with the highest probability in the PQ(MeOH) cluster. The PT character of the reactions is suggested by nonexistence of crossings between $\pi\pi^*$and $\pi\sigma^*$ states.

2. Executive Summary

We have carried out the dynamics simulations of ultrafast excited-state multiple intermolecular proton transfer (PT) reactions in some interesting systems such as 1*H*-pyrrolo[3,2-*h*]quinoline (PQ) with water and methanol ($PQ(H_2O)_n$ and $PQ(MeOH)_n$, where n = 1, 2), 7-azaindole (7AI) complexes with water, water-methanol and methanol, and $7AI(H_2O)_{1-5}$. The ground states of these target systems were optimized using quantum chemical calculations. The optimized ground states were further used in the excited-state dynamic simulation to obtain the dynamics information such as proton transfer pathway, corresponding time constants, and proton transfer probability. The results from these simulations have shed the light of solvent effect on excited-state proton transfer which is very important in chemistry and biological systems. The proton transfer pathway was confirmed by the non-crossing of two excited-states. The proton transfer times were found to be very rapid within sub-picoseconds in the gas-phase. However, the much slower proton transfer times might be observed in solution which is our further work based on current knowledge obtained from this study. The excited-state intramolecular proton transfer was also studied, however more comprehensive plans and better representative of interesting system must be proposed. So in this report, only excited-state proton transfer was reported. Our ongoing work on excited state intramolecular proton transfer has been carried out in our research group.

The knowledge that we have earned from this report under supported by TRF has helped our research group not only a change to study the basis science but also initiated a lot of national and international collaborations. This TRF grant has given a great opportunity to thai young researchers and also graduate students.

More complicated and interesting simulation on non-adiabatic systems and also nuclear quantum effect of 7AI dimer as well as 7AI dimer with waters are currently being carried out in our research group.

3. Objectives

1. To investigate the photoinduced tautomerization of proton transfer reactions in cyclic hydrogen-bonded $PQ(H_2O)_n$ and $PQ(MeOH)_n$ (n=1,2) complexes in the lowest-excited singlet state.

2. To determine the corresponding time constants of proton transfer process and also the mechanistic pathways of proton transfer in each complex of $PQ(H_2O)_n$ and $PQ(MeOH)_n$ (n=1,2).

3.To obtain the probabilities of the excited-state proton transfer processes in each of the complexes and to confirm the proton transfer character of the reactions on $PQ(H_2O)_n$ and $PQ(MeOH)_n$ (n=1,2).

4.To simulate the proton transfer dynamics of the $7AI(H_2O)_2$, $7AI(MeOH\text{-}H_2O)$, and $7AI(H_2O\text{-}MeOH)$ complexes.

5.To systematically study the role of different solvents surrounding 7AI, the effect of mixing solvents, and the influence of different connections at the proton donor site (pyrrole moiety).

Note: results of the objective 4 and 5 will be given in Appendix section

4. Research methodology

4.1 Introduction

The proton transfer (PT) is one of the most important classes of chemical reactions [1-2]. Because PT processes often take place within hydrogen-bonded systems, and because of the central role played by hydrogen bonds in chemistry and biology, a large number of studies have been performed on PT processes in both the ground and excited states [3-4]. A special class of compounds exhibiting PT is represented by heteroaromatic molecules [5-7]. In particular, heteroazaaromatic or bifunctional molecules having a hydrogen-bonding donor group (e.g., a pyrrole NH) and a hydrogen-bonding acceptor group (e.g., a quinoline-type N) are of great interests for their dual photochromic properties in a variety of solvents. Examples of molecules exhibiting intramolecular PT are salicylic acid and its derivatives [8]. Naturally, intramolecular PT will occur preferentially when the spatial separation between the donor and the acceptor sites is small [9-10]. In the case of a larger separation, the PT should proceed through a hydrogen-bond bridge established within a protic solvent. The phenomenon of phototautomerization is driven by a PT process in which the process may occur either in an intramolecular [11-14] or an intermolecular [5-7,9-10,15-17] manners. Thus, hydrogen bonding networks of these molecules with the solvent must be formed before molecules undergo excited-state proton transfer (ESPT). The heteroazaaromatic molecule requires a catalytic transfer via a one-molecule hydrogen-bonded proton-donor-acceptor bridge, or a two or more molecule PT relay [18]. There are many compounds belonging to the class of *N*-heteroazaaromatic molecules which undergo intermolecular PT. Those most studied are 7-azaindole (7AI) [5-7,9,15-17,19-20], 7-hydroxyquinoline (7HQ) [21-23], and 1-*H*-pyrrolo[3,2-*h*]quinoline (PQ or pyrido[3,2-*g*]indole) [7,24-28], For a general review on this topic see refs [7,29].

The structure of PQ can be viewed as similar to that of 7AI, modified by the addition of a benzo-ring spacer, separating the pyrido and the pyrrolo rings. Potentially valuable applications of PQ and its derivatives for chemical and biomedical uses have been reported [25-27,30-31]. For example, PQ was proposed as a host molecule in molecular recognition and as a potential anticancer drug [32]. It also exhibited bioactivity against tuberculosis and malaria [8]. In chemical applications, 1-methyl-pyrrolo[3,2]quinolone was found to be a good stabilizer for polymers [18]. Moreover, dipyridol[2,3-*a*:3 ,2 -*i*]carbazole (DPC) has been considered as a probe of hydrophilic/hydrophobic surface character [33]. To exhibit the photochemical activity necessary as a probe, PQ and its derivative must form hydrogen bonds with protic solvent partners.

Obviously, the geometry of PQ (Fig. 1) favors an internal hydrogen bond between the pyrrole NH and the pyridine N atom. PQ can, however, instead form a hydrogen-bonded network with solvent

partners, especially water and alcohols. Different stoichiometries of hydrogen-bonded complexes of PQ with water and methanol have been reported based on molecular dynamics simulations and density functional theory (DFT) [30,34]. 1:1 (doubly hydrogen-bonded) and 1:2 (triply hydrogen-bonded) cyclic complexes have been predicted to exist at low solvent concentrations and such complexes also existed in bulk solvent [34]. Both cyclic and non-cyclic hydrogen-bonded complexes have been determined. For $PQ(MeOH)_2$ complexes, DFT studies have shown that cyclic hydrogen-bonded species are more stable than non-cyclic ones. For PQ complexed with bulk water, the population of the 1:1 cyclic complex was found to be 3.5 times smaller than that of the cyclic complex in bulk methanol. A 1:2 complex, in which two water molecules form a cyclic hydrogen bonding network connecting the pyrrole N-H and the pyridine N atoms, has also been reported in studies combining infrared/femtosecond multiphoton ionization (IR/fsMPI) with fluorescence-detected infrared (FDIR) spectrometry associated with DFT calculations [24,27]. In such a cyclic hydrogen-bonded complex, triple PT through water bridges is possible upon excitation. The photophysics of jet-isolated complexes of PQ with water [27] and methanol [26] depends strongly on the cluster size. Complete lack of fluorescence was observed for the 1:1 complex, which has been justified by a fast ESPT reaction. Competing tautomerization as a result of the 1:2 complex might also contribute to the lack of fluorescence. The PT mechanism has previously been investigated by static calculations on the PQ with water and methanol complexes [26-27]. To the best of our knowledge, there are no previous reports on the dynamics of PT in the excited-state. Thus, to provide a more complete picture of ESPT in PQ-solvent complexes, dynamic simulations are required.

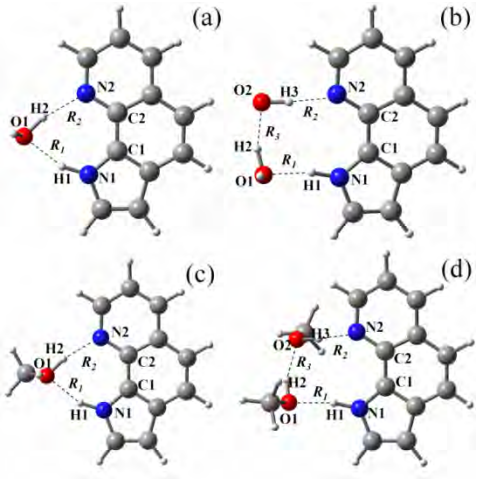

Figure 1. The ground-state optimized structures of $PQ(H_2O)_n$ and $PQ(MeOH)_n$ (n = 1,2) complexes at the RI-ADC(2)/SVP level. Atom numbering for intermolecular hydrogen bonds to water and methanol molecules (a) $PQ(H_2O)$ (b) $PQ(H_2O)_2$ (c) PQ(MeOH) and (d) $PQ(MeOH)_2$. Intermolecular hydrogen-bonded interactions are presented by dashed lines.

The aim of our work is to investigate the photoinduced tautomerization mechanism of PT reactions in cyclic hydrogen-bonded $PQ(H_2O)_n$ and $PQ(MeOH)_n$ (n = 1, 2) complexes in the lowest-excited singlet state. The methodology which we employ here, using the resolution-of-the-identity approximation for the electron repulsion integrals and algebraic diagrammatic construction through a second order method (RI-ADC(2)), was recently successfully applied by us to investigations of 7AI complexed with methanol molecules [9]. The goals of the present simulations are to determine the corresponding time constants of PT process and also the mechanistic pathways of PT in each complex. The probabilities of the ESPT processes in each of the complexes will be analyzed and compared. The PT character of the reactions will be also addressed in this work.

4.2 Computational details

4.2.1 Ground-State Calculations

Ground-state optimizations of $PQ(H_2O)_{n=1,2}$ and $PQ(MeOH)_{n=1,2}$ complexes were performed in the gas phase using the RI-ADC(2) [35-36] and the SVP [37] basis set, implemented in the TURBOMOLE 5.10 program package [38]. The minimum energy characters of all optimized structures were confirmed by normal mode analysis. These optimized structures were also used in excited-state dynamics simulations as explained below.

4.2.2 Excited-State Dynamics Simulations

Molecular dynamics simulations were carried out for the $PQ(H_2O)_{n=1,2}$ and $PQ(MeOH)_{n=1,2}$ complexes on the energy surface of the first excited state (S_1). The initial conditions were generated using a harmonic-oscillator Wigner distribution [39] for each normal mode, as implemented in the NEWTON-X program package [40-41] interfaced with the TURBOMOLE program. To reduce the computational cost, RI-ADC(2) with the SVP mixed SV(P) basis sets were employed. The SVP-SV(P) basis set is defined by assigning the split valence polarized SVP basis set to heavy atoms and hydrogen atoms involved in the hydrogen-bonded network of a complex, and using the split valence SV(P) basis set for the remaining hydrogen atoms. This small but sufficiently accurate mixed basis set has been tested and used in both static and dynamics calculations reported in our previous studies [9,14,42]. Fifty trajectories for each complex were simulated using a time step of 1 fs throughout the simulations, each of these having a total duration of 300 fs. Molecular orbital characterizations of the different electronic transitions were performed to verify the character of reactions. Furthermore, a statistical analysis was also carried out to give detailed properties (e.g. energies and internal coordinates), which were used to obtain time evolution of the transfer reactions along the hydrogen-bonded network.

5. Results and Discussion

5.1 Ground-State Structures

The optimized structures of PQ with water and methanol complexes, with important atoms belonging to intermolecular hydrogen-bonded networks numbered, are shown in Fig. 1. To understand the surrounding cooperative effect of water and methanol molecules on the hydrogen bonds of the complexes, the ground-state structures of $PQ(H_2O)_{n=1,2}$ and $PQ(MeOH)_{n=1,2}$ complexes with cyclic hydrogen-bonded network were optimized at the RI-ADC(2)/SVP-SV(P) level. The intermolecular hydrogen bonds (dashed lines) are characterized in TABLE 1.

TABLE 1: Summary of the ground-state structures computed at RI-ADC(2)/SVP level. Distances in Å, dihedral angles (□ N1C1C2N2 and ∠O1N1N2O2) in degrees.

	Complex			
	$PQ(H_2O)$	**$PQ(H_2O)_2$**	**PQ(MeOH)**	**$PQ(MeOH)_2$**
R_1	1.814	1.786	1.794	1.743
			(1.872)[a]	(1.765)
R_2	1.866	1.794	1.820	1.755
			(1.835)	(1.786)
R_3		1.750		1.720
				(1.762)
N1–O1	2.804	2.807	2.776	2.775
O[b]–N2	2.822	2.775	2.778	2.740
O1–O2		2.694		2.656
ø	5.2	2.9	-4.5	2.4
∠		-20.3		-33.4

[a] RI-MP2 level [26] for PQ with methanol in parentheses, [b] O1 for one water or methanol, O2 for two water or methanol molecules

5.1.1 $PQ(H_2O)_{n=1,2}$

When one water molecule is added to PQ, a cyclic hydrogen-bonded complex is formed (Fig. 1a). There are two intermolecular hydrogen bonds labeled as R_1(O1···H1), with a bond length of 1.814 Å, and R_2(N2···H2), with a bond distance of 1.866 Å. For two water molecules, there are three hydrogen bonds (Fig. 1b). The first one, between the oxygen atom of the first water and the hydrogen atom of the pyrrole ring (R_1(O1···H1)), has a bond length of 1.786 Å, slightly shorter than that of the equivalent bond in $PQ(H_2O)$. The second hydrogen bond, formed between the hydrogen atom of the second water and the pyridine N atom (R_2(N2···H3)), has a bond length of 1.794 Å, also shorter than that in $PQ(H_2O)$. The third hydrogen bond (R_3(O2···H2)) is formed between the two waters and it has a length of 1.750 Å.

5.1.2 $PQ(MeOH)_{n=1,2}$

When one methanol molecule is added to PQ, a cyclic hydrogen-bonded complex is formed similarly as in $PQ(H_2O)$. The PQ(MeOH) complex with relevant labels is shown in Fig. 1c. There are two hydrogen bonds in this complex: first, between the oxygen atom from methanol and the hydrogen from the pyrrole group (1.794 Å); second, between the hydrogen atom of methanol and the pyridine N atom (1.820 Å). The present RI-ADC(2) value for R_1 is shorter than the R_1 value computed at the MP2 level [26] by 0.08 Å. Values of R_2 computed with RI-ADC(2) and MP2 agree within 0.01 Å.

Starting from the PQ(MeOH) complex, a second methanol can be added. A cyclic intermolecular hydrogen-bonded network is formed with three hydrogen bonds (Fig. 1d). The first one, between the oxygen atom and the hydrogen atom of the pyrrole ring (R_1(O1···H1)), has a bond length of 1.743 Å, which is slightly shorter than the equivalent bond in $PQ(H_2O)$. The second hydrogen bond links the hydrogen atom of methanol to the pyridine N atom of PQ (R_2(N2···H3)) with a bond length of 1.755 Å. The third hydrogen bond, formed by the interaction between the two methanol molecules (R_3(O2···H2)), has a bond length of 1.720 Å. The present RI-ADC(2) values for R_1 and R_2 are in good agreement with the MP2 values reported in ref [26]. However, we calculate a value of R_3 shorter than that determined at the MP2 level by about 0.04 Å.

Generally, complexes of PQ with water and methanol form similar structures with hydrogen-bonded network. Either with water or methanol, the larger number of solvent molecules increases the strength of the hydrogen bonding network, as can be seen from the systematic shortening of R_1 and R_2 with the increase of the cluster size. However, the differences between them are governed by the methyl group of methanol. For the 1:2 complex of PQ, the water bridge gives a more planar hydrogen-bonded network than the methanol. The characteristic O1N1N2O2 dihedral angles in the ground state

are 20.3 and 33.4 degrees for the water and methanol complexes, respectively. The difference between these dihedral angles may be caused by the interaction between the methyl group of methanol and the PQ molecule.

5.2 Excited-State Dynamics Simulation

Fifty trajectories with different initial conditions were computed for each complex. Carrying simulation times out to 300 fs should reveal the entire mechanisms, including pre- and post-transfer processes. The trajectories for $PQ(H_2O)_{n=1,2}$ and $PQ(MeOH)_{n=1,2}$ complexes were analyzed and classified into three different types of reactions: (1) “ESPT”, when a proton (or hydrogen) is transferred within the simulation time; (2) “IC”, when an $S_1(\pi\pi^*)/S_0$ crossing is reached within the simulation time suggesting that internal conversion should take place; and (3) “No transfer” (NT), when no proton transfer occurs within the simulation time. The number of trajectories following each type of reaction, the PT probability, and the average transfer time for each complex are summarized in TABLE 2.

TABLE 2: Summary of the excited-state dynamics at RI-ADC(2)/SVP-SV(P) level of $PQ(H_2O)_{n=1,2}$ and $PQ(MeOH)_{n=1,2}$ complexes. Average distances (in Å) for PT time in parentheses.

Complex	Number of trajectories			ESPT Probability	Time (fs)		
	ESPT ($\pi\pi^*$)	IC ($\pi\pi^*/S_0$)	NT		PT1	PT2	PT3
$PQ(H_2O)$	12	7	31	0.24	75 (1.32)	82 (1.33)	
$PQ(H_2O)_2$	3	8	39	0.06	58 (1.28)	60 (1.32)	69 (1.27)
PQ(MeOH)	36	13	1	0.72	87 (1.32)	92 (1.32)	
$PQ(MeOH)_2$	14	10	26	0.28	61 (1.29)	64 (1.28)	67 (1.31)

The PT time is given as the time when the bond-breaking distance averaged over all trajectories exhibiting PT intersects the average bond-forming distance. This is the same definition that we have

used in our previous investigations [9,14,42]. The proton transfer mechanism can be assigned as either synchronous, concerted or stepwise depending on the delay time between two consecutive PTs [43]. If the delay time is shorter than about 10—15 fs, which corresponds to a vibrational period of N—H and O—H stretching modes, the PTs are synchronous, otherwise they are either concerted (a single kinetic step) or stepwise (two distinct kinetic steps via a stable intermediate).

To determine whether an excited-state proton transfer (PT) and/or an excited-state hydrogen atom transfer (HT) takes place during the dynamics, the relative energies of the ground (S_0) and the two lowest excited states ($\pi\pi^*$ and $\pi\sigma^*$) were computed along characteristic points of one single selected trajectory for each complex. These characteristic points are the complex at time 0 (normal or N), the intermediary structure (IS1 and IS2), and the tautomer structure (T). The IS1 and IS2 point were taken as the geometry when the hydrogen is midway between the donor and the acceptor atoms: IS1 as midway between the pyrrole NH of PQ and water, and IS2 as midway between water and the pyridine N of PQ. The T point was selected right after the transfer process was complete. The energies for each of these points (relative to the N point) are computed. Note that energies given in this table were computed for a single selected trajectory; therefore, they should not be taken as true energy barriers occurring on the energy surface. They provide, however, a qualitative picture of the reaction. For PQ(H_2O), these values are shown in the potential-energy diagram of Fig. 2.

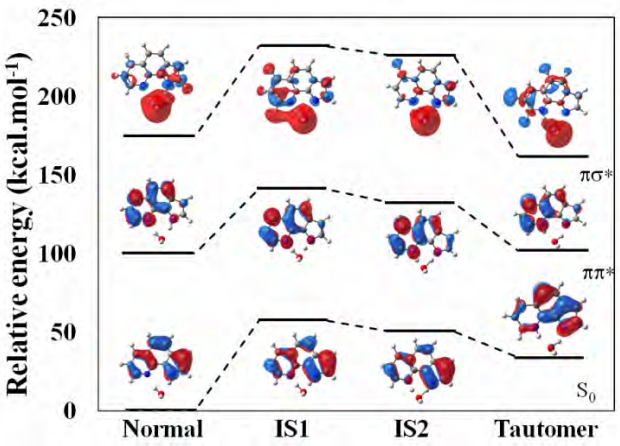

Figure 2. Potential-energy diagram of the ground state (S_0) and excited states ($\pi\pi^*$, $\pi\sigma^*$) of a selected trajectory for the PQ(H_2O) complex.

The main molecular orbitals involved in the excited states are also shown for each geometry in Fig. 2. The molecular orbital near S_0 is doubly occupied in the ground state. Upon excitation, it donates an electron to one of the orbitals pictured near the excited states. For instance, for the Normal structure in

Fig. 2, the first excited state corresponds to a $\pi\pi^*$ excitation, while the second excited state corresponds to a $\pi\sigma^*$ excitation. The π and the π^* orbitals are completely localized on PQ whereas the σ^* orbital is delocalized over PQ and the water molecule (Fig. 2). These features are independent of the geometry and also hold for the other complexes. The only exception is the σ^* orbital in $PQ(MeOH)_2$, which is mostly localized on the solvent molecules.

The relative energies of the $\pi\pi^*$ and $\pi\sigma^*$ states along the transfer pathway play an important role in determining the nature of the excited-state reaction, since PT should occur in the $\pi\pi^*$ state, whereas the HT should occur in the $\pi\sigma^*$ state [27,44-45]. The results for $PQ(H_2O)$ from Fig. 2 show that, first, there is no crossing between $\pi\pi^*$ and $\pi\sigma^*$ and that, second, $\pi\sigma^*$ lies well above $\pi\pi^*$. This implies that the dynamics along the first excited state takes place purely in the $\pi\pi^*$ state, characterizing a PT process. The same feature holds for the other three complexes.

5.2.1 $PQ(H_2O)$ complex

On-the-fly dynamics simulations were carried out for 50 trajectories of the $PQ(H_2O)$ complex. A total of 12 trajectories showed excited-state double proton transfer (ESDPT) (24% probability, TABLE 2). The PT process did not occur in 31 trajectories during the simulation time. Seven trajectories reached a small energy gap between S_1 and S_0 (< 0.5 eV) and could not be continued because of limitations of RI-ADC(2) in dealing with such multireference regions of the potential energy surface. Back-PT reaction was also observed in some trajectories. The structures along the reaction pathway are depicted in Fig. 3 for a selected trajectory. The PT process, indicated by an arrow, can be described by the following events: First, a normal (N) form is observed at time 0. Second, the first proton (H1) moves from N1 on the pyrrole ring to the O1 atom (PT1) at 72 fs, then the second proton (H2) of water moves to N2 on pyridine (PT2) at 76 fs (see atom numbering in Fig. 1). Finally, the tautomer (T) form is formed within 85 fs. After the tautomerization with water assistance is completed, PQ and water fragments dissociate.

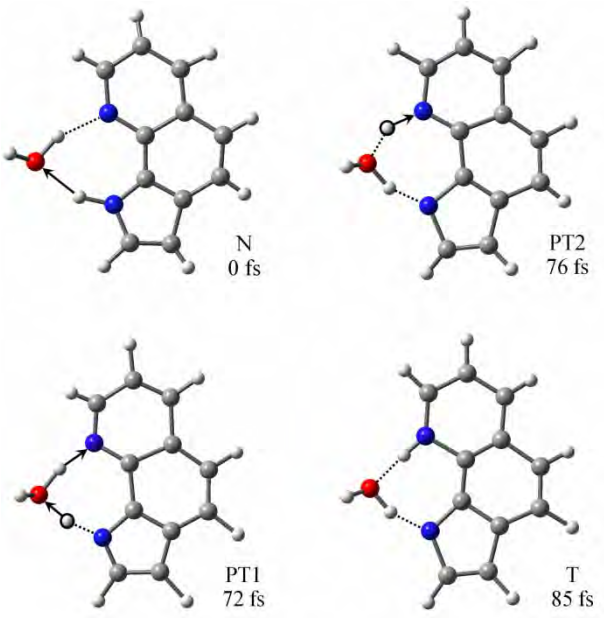

Figure 3. Snapshots from a selected trajectory of the PQ(H_2O) dynamics showing the time evolution of the ESDPT reaction through the hydrogen-bonded network within 85 fs. Normal (N), Proton transfer (PT), and Tautomer (T).

The time evolution of the two bond-forming distances O1···H1 and N2···H2 and of the two bond-breaking distances N1–H1 and O1–H2 along the PT pathway of the ESDPT process averaged over the 12 trajectories are shown in Fig. 4a. Along the dynamics, the two bond-forming distances decrease to covalent bond length, whereas the two bond-breaking distances increase. At 75 fs, the average values of N1···H1 and O1···H1 bond distances are equal (1.32 Å), which indicates the time for the PT1 process. The second PT occurs at 82 fs, since at this time the average bond distances of O1···H2 and N2···H2 are equal (1.33 Å). After 150 fs, the O1–H1 and the N2–H2 distances start to exhibit oscillations around their equilibrium values. The interval time of about 7 fs between first and second PT implies that the process is a concerted synchronous PT. The average times are summarized in TABLE 2.

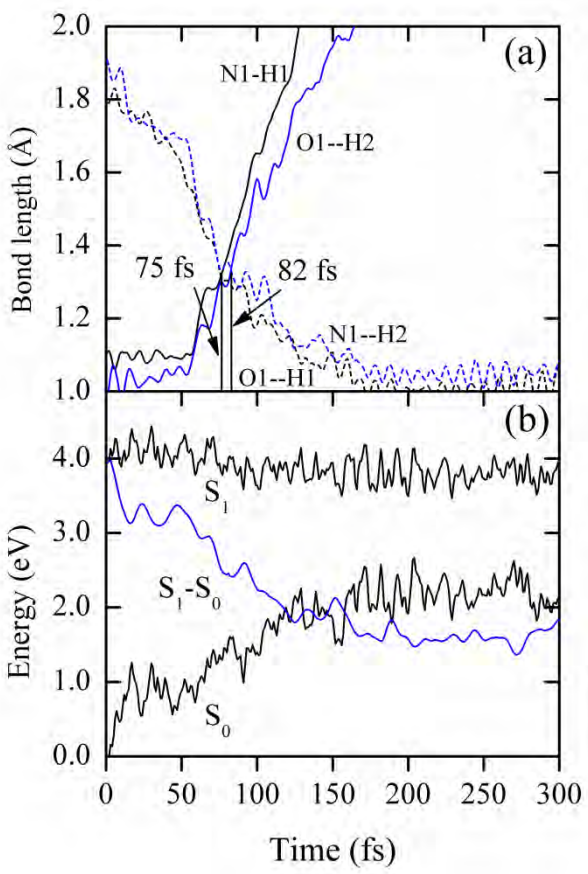

Figure 4. Average properties over the 12 trajectories of the PQ(H_2O) complex exhibiting ESDPT, as a function of time: (a) Average lengths of broken and new bonds; (b) Average relative energies of the excited state (S_1), ground state (S_0), and the S_1-S_0 energy gap.

The time evolution of the ground and excited state energies averaged over the same 12 trajectories exhibiting ESDPT is shown in Fig. 4b. The average S_1-S_0 energy gap gradually decreases during the first 120 fs. After that, the average energy gap is still close to 2 eV, indicating that the structure of PQ tends to be planar throughout the process [46]. This planarity of the PQ skeleton is confirmed by the average value of the torsion angle N1C1C2N2, which remains around 180º throughout the simulation time.

5.2.2 PQ(H_2O)$_2$ complex

From 50 trajectories computed for the PQ(H_2O)$_2$ complex, three exhibited excited-state triple proton transfer (ESTPT) (6% probability, TABLE 2). The PT process did not occur for 39 trajectories during the simulation time. Eight trajectories reached a region of internal conversion (crossing between the $\pi\pi^*$ and S_0 states). The details of the PT process can be seen in the selected trajectory pictured in

Fig. 5. A normal (N) form is observed at time 0. The first proton (H1) leaves the pyrrole ring, moving towards the O1 atom (PT1) at 54 fs. The PT2 occurs at 66 fs when the second proton (H2) of water moves to the O2 acceptor of the second water, and, at the same time, the PT3 also takes place as the third proton (H3) moves from the second water to the N2 on pyridine. Completion of the ESTPT reaction is reached after 71 fs and followed by the separation of PQ and water fragments.

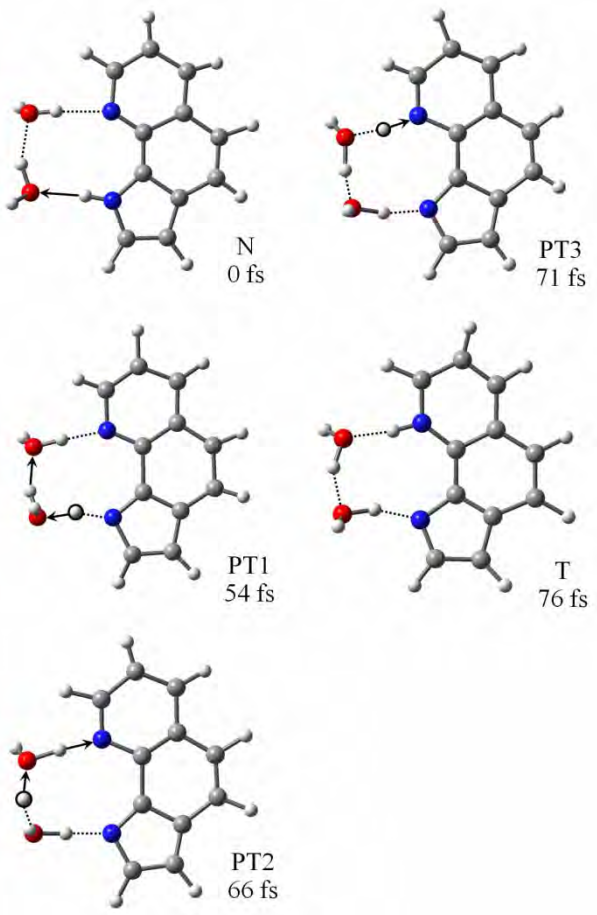

Figure 5. Snapshots from a selected trajectory of the PQ$(H_2O)_2$ complex showing the time evolution of the ESTPT reaction through the hydrogen-bonded network, occurring within 76 fs.

The time evolution of the three bond-breaking distances (N1–H1, O1–H2, and O2–H3) and of the three bond-forming distances (O1···H1, O2···H2, and N2···H3) averaged over the three trajectories exhibiting PT was computed. Along the trajectories, the first PT occurs at 58 fs (N1···H1 and O1···H1 are equal to 1.28 Å) and the occurrences of the second PT (O1···H2 and O2···H2 equal to 1.32 Å) and of the third PT (O2···H3 and N2···H3 equal to 1.27 Å) are observed at 60 and 69 fs, respectively. This dynamic behavior is considered as a concerted synchronous PT process. Fig. S4b shows that the S_1–S_0 energy gap gradually decreases in the first 100 fs. After that, the energy gap is still around 2 eV, indicating that the PQ skeleton remains planar during the simulation time.

5.2.3 PQ(MeOH) complex

The ESDPT reaction occurred in 36 out of 50 trajectories (72% probability, TABLE 2), while no reaction was observed in one trajectory, and 13 trajectories reached the region of internal conversion. Snapshots for a selected trajectory are shown in Fig. 6. Beginning with the normal form (N) at time 0, the PT process is described in the following steps: First, the first proton (H1) moves from the pyrrole ring to the O1 atom (PT1) at 72 fs; then, the second proton (H2) of the methanol moves to the N2 in pyridine (PT2) at 79 fs. Finally, the tautomer (T) formation is complete with the assistance of methanol at 85 fs. After the tautomerization, the PQ and methanol fragments dissociate as in the case of the PQ(H_2O) complex.

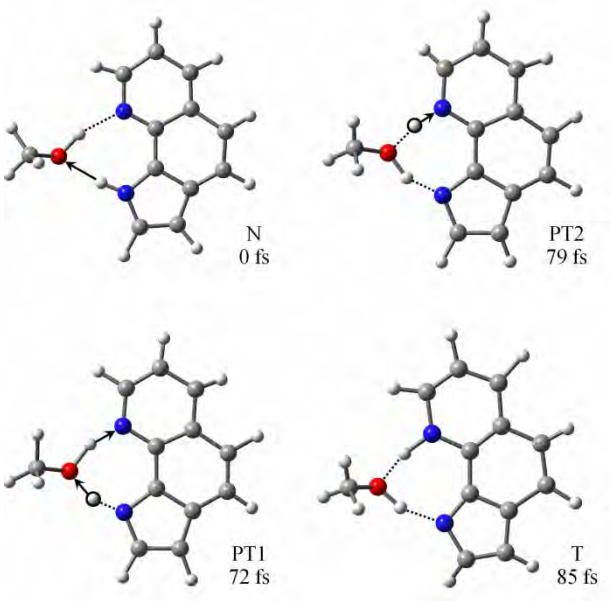

Figure 6. Snapshots from a selected trajectory of the PQ(MeOH) dynamics showing the time evolution of the ESDPT reaction through the hydrogen-bonded network, occurring within 85 fs.

The time evolution of the two bond-breaking distances (N1–H1 and O1–H2) and of the two bond-forming distances (O1···H1 and N2···H2) along the hydrogen-bonded network of the ESDPT process averaged over the 36 trajectories exhibiting ESDPT are computed. The intersection between the curves indicates that the first and second PT processes occur at 87 and 92 fs, respectively. This dynamic behavior indicates a concerted synchronous process. As in the previous cases, the S_1-S_0 energy gap gradually decreases in the first 100 fs. After that, the average energy difference is always slightly below 2.0 eV revealing that no approach to a conical intersection between the two states is reached within the simulation time.

5.2.4 $PQ(MeOH)_2$ complex

The ESTPT reaction occurred in 14 trajectories (28%, TABLE 2), while no reaction was observed in 26 trajectories within the simulation time. Ten trajectories reached a crossing region between the S_1 and S_0. The dynamic details of the PT process for a selected trajectory are illustrated in Fig. 7. Starting with the normal structure (N) at time 0, the complete process follows the following three steps: (1) the first proton (H1) moves from N1 to O1 (PT1) at 56 fs, (2) the second proton (H2) moves from the O1 of the first methanol to the O2 of the second methanol (PT2) at 60 fs, and (3) the third proton (H3) moves from O2 to N2 (PT3) starting at 63 fs until the methanol-assisted tautomerization (T) is completed. The complete ESTPT reaction is reached after 70 fs and followed by the separation of PQ and MeOH fragments.

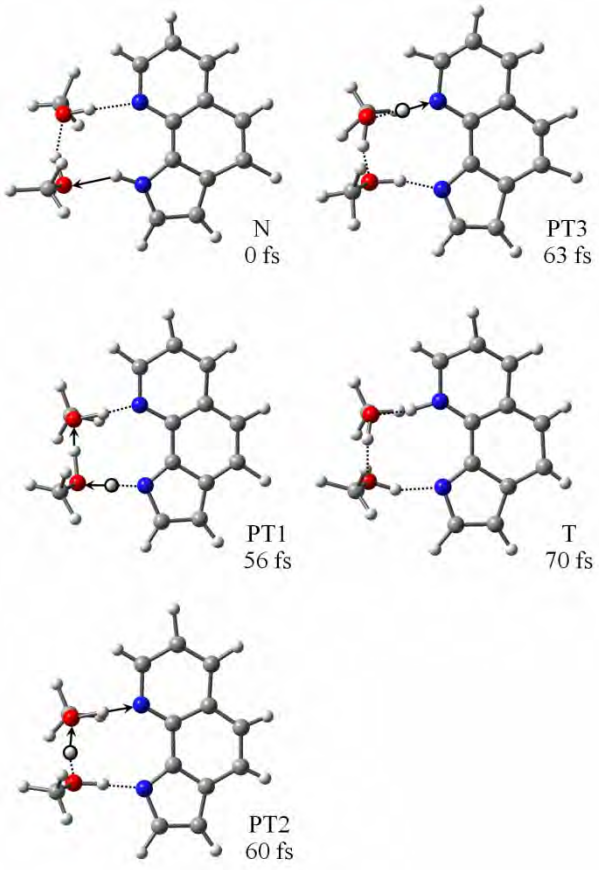

Figure 7. Snapshots from a selected trajectory of the $PQ(MeOH)_2$ dynamics showing the time evolution of the ESTPT reaction through the hydrogen-bonded network, occurring within 70 fs.

The time evolutions of the three bond-breaking distances (N1–H1, O1–H2, and O2–H3) averaged over the 14 trajectories exhibiting ESTPT show steep increases, and simultaneously, the time evolutions of the bond-forming distances (O1···H1, O2···H2, and N2···H3) show steep decreases. The first PT process occurs at 61 fs when the average O2···H3 and N2···H3 distances are equal (1.29 Å). The

second proton transfers from the PQ molecule to the first methanol at 64 fs when the average N1···H1 and O1···H1 distances are both equal to 1.28 Å. The last PT occurs at 67 fs when the average O1···H2 and O2···H2 distances are equal (1.31 Å). Once more, the PT processes are concerted synchronous. The S_1–S_0 energy gap behaves like in the previous cases, with stabilization around 2 eV.

5.2.5 Comparative analysis

For all trajectory of complete ESPT of each complex, we computed the average energies of (S_0) and the first-excited ($\pi\pi^*$) states for the normal (N), intermediary (IS1, IS2, and IS3 (only complexes of PQ with two water and two methanol molecules)), and tautomer (T) structures along the reaction pathway as shown in figure 8. The results show that the average excited-state reaction path has barriers of 3 and 8 kcal.mol^{-1} for the PQ(H_2O) and PQ(H_2O)$_2$, while it is barrierless for PQ(MeOH) and PQ(MeOH)$_2$. The average excited-state barriers correlate well with the PT probability reported in TABLE 2. In particular, it supports why the probability of the PT reaction increases from 24% to 72% in the comparison between PQ(H_2O) and PQ(MeOH). The increase in the probability of PT between PQ(H_2O)$_2$ and PQ(MeOH)$_2$ from 6% to 28% is also rationalized. Moreover, the larger excited-state barrier for PQ(H_2O)$_{1\text{-}2}$ than for PQ(MeOH)$_{1\text{-}2}$ is in good agreement with calculated results [24] and LIF excitation spectrum [26].

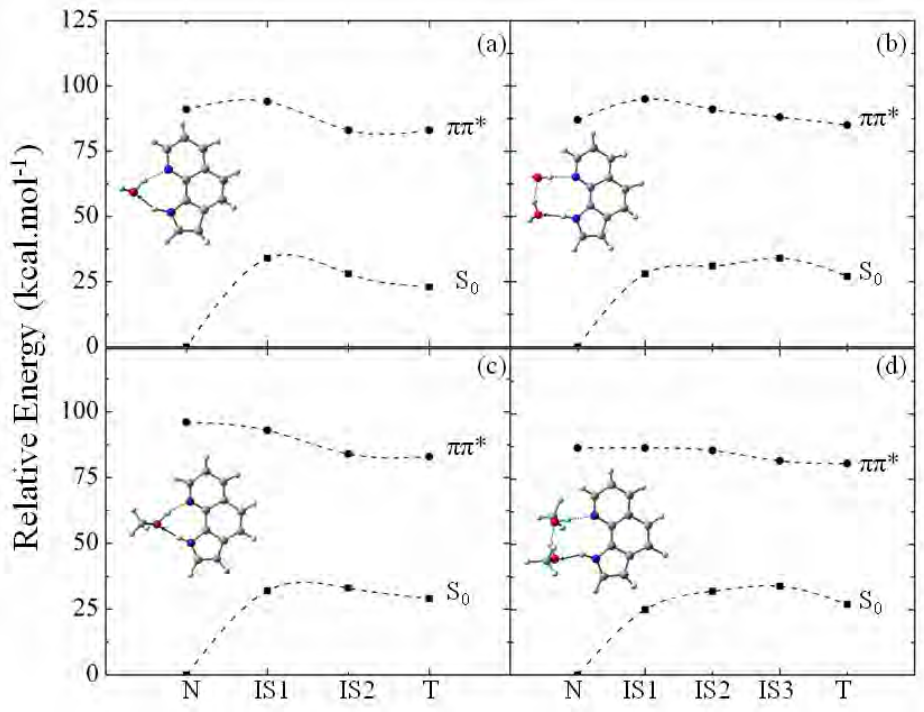

Figure 8. Average Relative energies (kcal.mol^{-1}) of the ground (S_0) and the excited states ($\pi\pi^*$) of (a) PQ(H_2O), (b) PQ(H_2O)$_2$, (c) PQ(MeOH), and (d) PQ(MeOH)$_2$ complexes.

For the PT time evolution, all complexes share a common pattern: after photoexcitation, it takes a relatively long time to initiate the PT process, between 58 and 87 fs (TABLE 2). However, as soon as the first PT is initiated, it triggers a fast sequence of proton transfers through the solvent bridge, until tautomerization is achieved within 92 fs. The delay between each PT is always under 9 fs, characterizing a concerted synchronous process. Independently of the solvent, the time for the first PT in PQ-solvent clusters is longer than that in HBT in water (10 fs), [14] but similar to those predicted for 7AI in methanol (57-71 fs) [9].

Our results clearly reveal that the initial PT time for PQ in water is slightly shorter than that in methanol about 10 fs. For n = 1, these times are 75 and 92 fs, whereas for n = 2, they are 58 and 69 fs. The delay times between each PT for PQ with one and two water molecules were found to be longer than those of PQ with one and two methanol molecules; however, they are still characteristics of concerted synchronous processes. The complete PT time decreases from 92 fs to 67 fs for PQ with water and from 92 fs to 67 fs for PQ with methanol when increasing the number of participating solvent molecules from one to two. This slight difference might be explained by the strength of hydrogen bond (HB) in PQ with more solvent molecules upon photoexcitation, which is stronger in the case of two solvent molecules compared to one solvent molecule (see values in TABLE 2) resulting in a faster complete PT time. In the case of PQ(H_2O), its early starting of the first PT (compared to PQ(MeOH)) together with the planarity of its O1N1N2O2 dihedral angle contributes to a completion of the tautomerization process 10 fs faster than that in PQ(MeOH).

Our results show that the ESmultiPT process of PQ with water and methanol is cluster-size selective. The stoichiometry of 1:1 complexes exhibits higher efficiency than that of 1:2 complexes for both solvents, as revealed by the PT probabilities. In particular, one single methanol molecule seems to facilitate the tautomerization reaction most effectively among all investigated complexes.

6. Conclusion

The ground-state structures of PQ$(H_2O)_{n=1,2}$ and PQ$(MeOH)_{n=1,2}$ complexes at the RI-ADC(2)/SVP level were investigated. It was found that intermolecular hydrogen bonds of PQ with water and methanol become stronger when the number of solvent molecules increases. Excited-state dynamics simulations were performed to reveal details of the excited-state PT pathways for all reactions within PQ$(H_2O)_{n=1,2}$ and PQ$(MeOH)_{n=1,2}$ complexes. The excited-state proton transfer reactions are ultrafast processes depending on the cluster size. Phototautomerization of all complexes occurs in less than 92 fs. Moreover, the ESPT process was found to have a concerted synchronous mechanism for all complexes, with delay times between proton transfers always under 9 fs. Our

investigations also show that the intermolecular ESPT in the first excited state occurs along a pathway with $\pi\pi^*$ character, located within the π system of PQ, regardless of the solvent partner. No crossing between $\pi\pi^*$ and $\pi\sigma^*$ states is observed. Thus, these transfer processes are characterized as PT and not as HT.

References

1. Arnaut LG, Formosinho SJ (1993) J Photochem Photobiol A 75:1-20.

2. Formosinho SJ, Arnaut LG (1993) J Photochem Photobiol A 75:21-48.

3. Han K-L, Zhao G-J (2011) Hydrogen Bonding and Transfer in the Excited State, Volume II. vol Copyright (C) 2011 American Chemical Society (ACS). All Rights Reserved. John Wiley & Sons Ltd.,

4. Zhao G-J, Han K-L (2012) Acc Chem Res 45:404-413.

5. Gordon MS (1996) J Phys Chem 100:3974-3979.

6. Mente S, Maroncelli M (1998) J Phys Chem A 102:3860-3876.

7. Waluk J (2003) Acc Chem Res 36:832-838.

8. Reyman D, Díaz-Oliva C (2011) Excited-State Double Hydrogen Bonding Induced by Charge Transfer in Isomeric Bifunctional Azaaromatic Compounds. Hydrogen Bonding and Transfer in the Excited State, Volume I & II:661-709

9. Daengngern R, Kungwan N, Wolschann P, Aquino AJA, Lischka H, Barbatti M (2011) J Phys Chem A 115:14129-14136.

10. Sakota K, Jouvet C, Dedonder C, Fujii M, Sekiya H (2010) J Phys Chem A 114:11161-11166.

11. Filarowski A, Koll A, Hansen PE, Kluba M (2008) J Phys Chem A 112:3478-3485.

12. Filarowski A, Majerz I (2008) J Phys Chem A 112:3119-3126.

13. Jezierska-Mazzarello A, Vuilleumier R, Panek JJ, Ciccotti G (2010) J Phys Chem B 114:242-253.

14. Kungwan N, Plasser F, Aquino AJA, Barbatti M, Wolschann P, Lischka H (2012) Phys Chem Chem Phys 14:9016-9025.

15. Hara A, Sakota K, Nakagaki M, Sekiya H (2005) Chem Phys Lett 407:30-34.

16. Sakota K, Komoto Y, Nakagaki M, Ishikawa W, Sekiya H (2007) Chem Phys Lett 435:1-4.

17. Sakota K, Inoue N, Komoto Y, Sekiya H (2007) J Phys Chem A 111:4596-4603.

18. Taylor CA, El-Bayoumi MA, Kasha M (1969) Proc Natl Acad Sci USA 63:253-260.

19. Ilich P (1995) J Mol Struct 354:37-47.

20. Kina D, Nakayama A, Noro T, Taketsugu T, Gordon MS (2008) J Phys Chem A 112:9675-9683.

21. Fernández-Ramos A, Martínez-Núñez E, Vázquez SA, Ríos MA, Estévez CM, Merchán M, Serrano-Andrés L (2007) J Phys Chem A 111:5907-5912.

22. Guglielmi M, Tavernelli I, Rothlisberger U (2009) Phys Chem Chem Phys 11:4549-4555

23. Park SY, Jang DJ (2009) J Am Chem Soc 132:297-302.

24. Kyrychenko A, Waluk J (2006) J Phys Chem A 110:11958-11967.

25. Nosenko Y, Kunitski M, Thummel RP, Kyrychenko A, Herbich J, Waluk J, Riehn C, Brutschy B (2006) J Am Chem Soc 128:10000-10001.

26. Nosenko Y, Kyrychenko A, Thummel RP, Waluk J, Brutschy B, Herbich J (2007) Phys Chem Chem Phys 9:3276-3285.

27. Nosenko Y, Kunitski M, Riehn C, Thummel RP, Kyrychenko A, Herbich J, Waluk J, Brutschy B (2008) J Phys Chem A 112:1150-1156.

28. Gorski A, Gawinkowski S, Herbich J, Krauss O, Brutschy B, Thummel RP, Waluk J (2012) The Journal of Physical Chemistry A 116:11973-11986.

29. Wiosna G, Petkova I, Mudadu MS, Thummel RP, Waluk J (2004) Chem Phys Lett 400:379-383.

30. Kyrychenko A, Herbich J, Izydorzak M, Wu F, Thummel RP, Waluk J (1999) J Am Chem Soc 121:11179-11188.

31. Kyrychenko A, Herbich J, Wu F, Thummel RP, Waluk J (2000) J Am Chem Soc 122:2818-2827.

32. Ferlin MG, Chiarelotto G, Baccichetti F, Carlassare F, Toniolo L, Bordin F (1992) Farmaco 47:1513-1528.

33. Herbich J, Dobkowski J, Thummel RP, Hegde V, Waluk J (1997) J Phys Chem A 101:5839-5845.

34. Kyrychenko A, Stepanenko Y, Waluk J (2000) J Phys Chem A 104:9542-9555.

35. Hättig C (2003) J Chem Phys 118:7751-7761.

36. Hättig C (2005) Adv Quantum Chem 50:37-60.

37. Schäfer A, Horn H, Ahlrichs R (1992) J Chem Phys 97:2571-2577.

38. Ahlrichs R, Bär M, Häser M, Horn H, Kölmel C (1989) Chem Phys Lett 162:165-169.

39. Barbatti M, Aquino AJA, Lischka H (2010) Phys Chem Chem Phys 12:4959-4967.

40. Barbatti M, Granucci G, Ruckenbauer M, Plasser F, Pittner J, Persico M, Lischka H (2011) Newton-X: a package for Newtonian dynamics close to the crossing seam, version 12, wwwnewtonxorg.

41. Barbatti M, Granucci G, Persico M, Ruckenbauer M, Vazdar M, Eckert-Maksic M, Lischka H (2007) J Photochem Photobiol, A 190:228-240.

42. Barbatti M, Aquino AJA, Lischka H, Schriever C, Lochbrunner S, Riedle E (2009) Phys Chem Chem Phys 11:1406-1415.

43. Dewar MJS (1984) J Am Chem Soc 106:209-219.

44. Al-Lawatia N, Husband J, Steinbrecher T, Abou-Zied OK (2011) J Phys Chem A 115:4195-4201.

45. Tanner C, Manca C, Leutwyler S (2003) Science (Washington, DC, U S) 302:1736-1739.

46. Barbatti M, Aquino AJA, Lischka H, Schriever C, Lochbrunner S, Riedle E (2009) Phys Chem Chem Phys 11:1406-1415.

7. Appendix

1. Important activities related to this project and overseas collaborations initiated from this TRF grant
2. In press manuscript (7AI with water, water-methanol and methanol) and submitted manuscript which is being revised (PQ with water and methanol)

Important activities related to this project and overseas collaborations initiated from this TRF grant

1. Main organizer and also one of speakers in workshop and conference for 8th Thai Summer School of Computational Chemistry (8th TS_2C_2)
2. Oral presentation on excited-state intermolecular proton transfer reactions of 7-azaindole(MeOH)1-3 clusters in the gas phase: on the fly dynamic simulation at Mini symposium: Future of biomolecular simulations in life science applications in honor of 65th birthday anniversary of Prof. Dr. Peter Wolschan at Chulalongkron University on 1st December 2011.
3. Oral presentation on the effect hydrogen bonding on excited-state proton transfer in 7-azaindole in water (1 to 5 waters): theoretical study at The 5th TRF seminar research scholar annual meeting: Innovative research on Anti-AIDS drug discovery: Phase II in Nakornsriayunthaya on 28 July 2012.
4. Oral presentation on excited-state multiple proton transfer reaction of 7-azaindole (H_2O)1-5 clusters in the gas phase: hydrogen bond rearrangement and secondary shell effect at PACCON2013 in Pattaya, Chonburi organized by Burapha University on 23-15 January 2013.

Overseas collaborations initiated from this TRF grant

1. Dr. Mario Barbatti from Max-Plank-Institut fuer Kohlenforschung, Muelheim an der Ruhr, Germany (Mentor, started collaboration since 2009).
2. Prof. Stephan Irle from Nagoya University, Nagoya, Japan (started joining excited-state protron transfer projects since January 2013)
3. Prof. Masanori Tachikawa from Yokohama City University (started joining path integral molecular dynamics on 7-azaindole dimer and some interesting hydrogen bonded dimer since April 2013).

AUTHOR QUERY FORM

ELSEVIER	**Journal:** JPC **Article Number:** 9438	**Please e-mail or fax your responses and any corrections to:** **E-mail:** corrections.esch@elsevier.thomsondigital.com **Fax:** +353 6170 9272

Dear Author,

Please check your proof carefully and mark all corrections at the appropriate place in the proof (e.g., by using on-screen annotation in the PDF file) or compile them in a separate list. Note: if you opt to annotate the file with software other than Adobe Reader then please also highlight the appropriate place in the PDF file. To ensure fast publication of your paper please return your corrections within 48 hours.

For correction or revision of any artwork, please consult http://www.elsevier.com/artworkinstructions.

Any queries or remarks that have arisen during the processing of your manuscript are listed below and highlighted by flags in the proof. Click on the 'Q' link to go to the location in the proof.

Location in article	Query / Remark: click on the Q link to go Please insert your reply or correction at the corresponding line in the proof
Q1 Q2	Please confirm that given names and surnames have been identified correctly. Fig. 3 will appear in black and white in print and in color on the web. Based on this, the respective figure captions have been updated. Please check, and correct if necessary. Please check this box or indicate your approval if you have no corrections to make to the PDF file ☐

Thank you for your assistance.

Journal of Photochemistry and Photobiology A: Chemistry xxx (2013) xxx–xxx

Contents lists available at SciVerse ScienceDirect

Journal of Photochemistry and Photobiology A: Chemistry

journal homepage: www.elsevier.com/locate/jphotochem

Graphical Abstract

Journal of Photochemistry and Photobiology A: Chemistry xxx (2013) xxx–xxx

Dynamics simulations of excited-state triple proton transfer in 7-azaindole complexes with water, water–methanol and methanol

Rathawat Daengngern, Khanittha Kerdpol, Nawee Kungwan*, Supa Hannongbua, Mario Barbatti

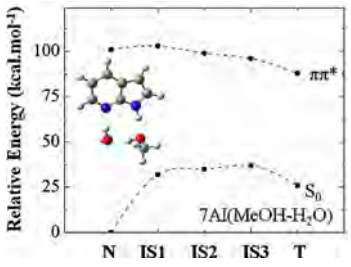

Journal of Photochemistry and Photobiology A: Chemistry xxx (2013) xxx–xxx

Contents lists available at SciVerse ScienceDirect

Journal of Photochemistry and Photobiology A: Chemistry

journal homepage: www.elsevier.com/locate/jphotochem

Highlights

Journal of Photochemistry and Photobiology A: Chemistry xxx (2013) xxx–xxx

Dynamics simulations of excited-state triple proton transfer in 7-azaindole complexes with water, water–methanol and methanol

Rathawat Daengngern, Khanittha Kerdpol, Nawee Kungwan*, Supa Hannongbua, Mario Barbatti

- We model excited-state triple proton transfer (ESTPT) of 7-azaindole with solvents.
- The PT from pyrrole to the solvent is the rate determining step of the ESTPT.
- The pathway is most likely a PT with no crossing between $\pi\pi^*$ and $\pi\sigma^*$ states.
- The ESTPT is ultrafast within 85 fs.

Journal of Photochemistry and Photobiology A: Chemistry xxx (2013) xxx–xxx

Contents lists available at SciVerse ScienceDirect

Journal of Photochemistry and Photobiology A: Chemistry

journal homepage: www.elsevier.com/locate/jphotochem

Dynamics simulations of excited-state triple proton transfer in 7-azaindole complexes with water, water–methanol and methanol

Rathawat Daengngern[a], Khanittha Kerdpol[a], Nawee Kungwan[a,*], Supa Hannongbua[b], Mario Barbatti[c]

[a] Department of Chemistry, Faculty of Science, Chiang Mai University, Chiang Mai 50200, Thailand
[b] Department of Chemistry, Faculty of Science, Kasetsart University, Bangkhen Campus, Bangkok 10930, Thailand
[c] Max-Planck-Institut für Kohlenforschung, Kaiser-Wilhelm-Platz 1, D-45470 Mülheim an der Ruhr, Germany

ARTICLE INFO

Article history:
Received 14 February 2013
Received in revised form 26 March 2013
Accepted 24 May 2013
Available online xxx

Keywords:
Dynamics simulation
Excited-state proton transfer
Excited-state tautomerization
Water–methanol mixture
7-Azaindole
ADC(2)

ABSTRACT

Excited-state triple proton transfer (ESTPT) reactions in 7-azaindole (7AI) complexed with two water, with one water and one methanol, and with two methanol molecules were investigated by dynamics simulations in the first excited state computed with the second order algebraic-diagrammatic construction (ADC (2)) method. The results show that photoexcitation may trigger ultrafast an asynchronous concerted proton transfer via two solvent molecules along an intermolecular hydrogen-bonded network. The probability of occurrence of ESTPT ranges from 32% for 7AI(H_2O–MeOH) to 64% for 7AI$(MeOH)_2$. The average time for completing the ESTPT varies between 58 and 85 fs depending on the complex. The proton transfer (rather than hydrogen transfer) nature of the reaction was suggested by the nonexistence of crossings between the $\pi\pi^*$ and $\pi\sigma^*$ states.

1. Introduction

Excited-state proton transfer (ESPT) [1,2] is one important class of reactions in physical, chemical and biological phenomena, with uses in fluorescent probes [3–5], photostabilizers [6] and light-emitting devices [7,8]. Among many molecules undergoing ESPT, 7-azaindole (7AI) has been the most widely investigated by experimental and theoretical techniques [9–36]. All this attention paid to 7AI is owned to its potential as a model system for studying ESPT phenomena in several instances, such as DNA mutagenesis, proton relay in enzymes, and proton transport through membranes [37]. A more complete understanding of the multiple proton transfer processes occurring in 7AI complexed with solvent partners may shed the light on the occurrence of these important phenomena.

7AI is a bicyclic azaaromatic molecule comprising a pyrrole (proton donor) and a pyridine (proton acceptor) rings (Fig. 1). The proton donor and proton acceptor sites can form a hydrogen-bonded network upon dimerization in nonpolar solvents and in complexation with protic solvents such as ammonia, water and alcohol. The excited-state tautomerization of 7AI within water has been intensively studied in the condensed and gas phases with experimental and theoretical methods [21,23,30,38–41]. The excited-state multiple proton transfers in 7AI complexed with alcohol has been also thoroughly studied [15,21,22,29,32,42]. Most previous theoretical studies related to 7AI, however, were focused only on static calculations either in the ground state or excited state. Therefore, these studies could not provide a time-dependent picture of the proton transfer (PT) or hydrogen transfer (HT) reaction pathways. (The nature of the transfer, whether it is a PT or HT, depends on the energy of the $\pi\pi^*$ and $\pi\sigma^*$ states, as PTs occur along the $\pi\pi^*$ state whereas HTs occur along the $\pi\sigma^*$ state [43,44]. We will show that for the 7AI complexes investigated here, PT most likely takes place.)

To the best of our knowledge, there has been no theoretical investigation reported on the intermolecular ESPT dynamics in 7AI within mixed solvents such as water–methanol. 7-Hydroxyquinoine (7HQ) with mixed ammonia/water solvent-wire clusters was reported by Tanner et al. [44–46]. Their results showed that replacing NH_3 molecule with one or two water molecules stopped the hydrogen-atom transfer along the solvent wires. For 7AI with water, Kina et al. [40] performed dynamics simulations at the CASSCF level to study complexes with up two water molecules and simulations at the CASSCF/MM level to investigate water solvation effects. Their results showed that the complete ESIPT process was reached around 50 fs in 7AI(H_2O) and in the range of 40–60 fs

* Corresponding author. Tel.: +66 53 943341x101; fax: +66 53 892277.
E-mail addresses: naweekung@gmail.com, naweekung@hotmail.com (N. Kungwan).

1010-6030/$ – see front matter © 2013 Elsevier B.V. All rights reserved.
http://dx.doi.org/10.1016/j.jphotochem.2013.05.012

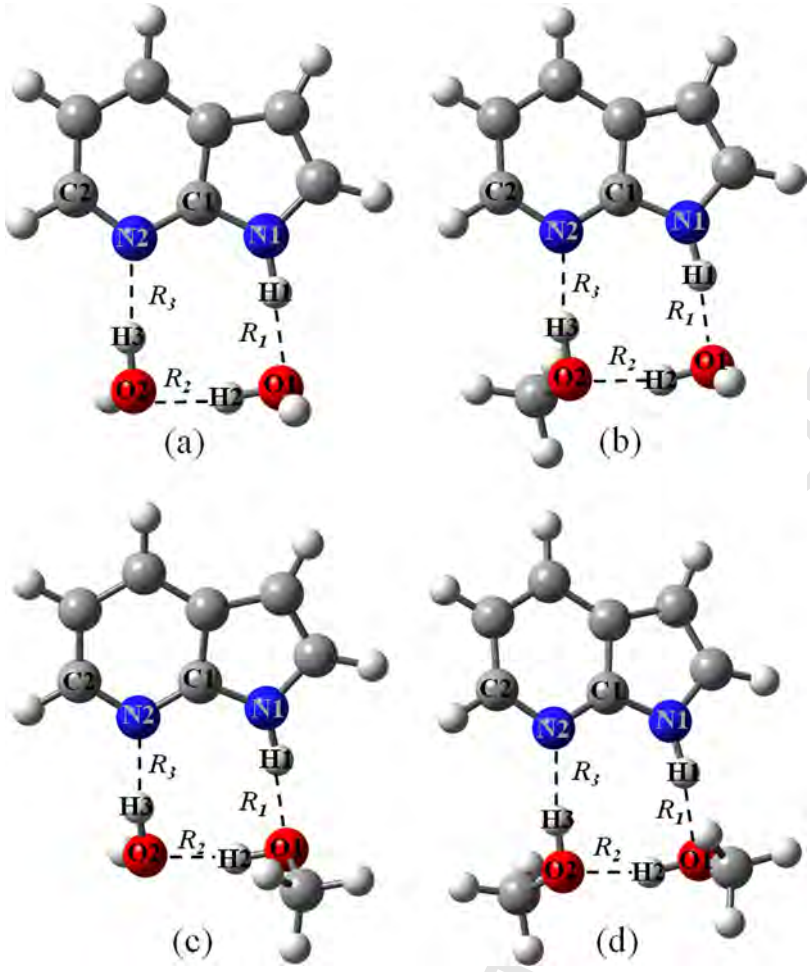

Fig. 1. Ground-state optimized structures of 7AI complexes at RI-ADC(2)/SVP-SV(P) level: (a) 7AI$(H_2O)_2$, (b) 7AI(H_2O–MeOH), (c) 7AI(MeOH–H_2O), and (d) 7AI$(MeOH)_2$. Intermolecular hydrogen bonds are indicated by dashed lines.

in 7AI$(H_2O)_2$ cluster. Another recent investigation using on-the-fly dynamics simulation was done by our group [20] on the excited-state multiple proton transfer reaction in the gas phase cluster of 7AI$(MeOH)_n$ (n = 1–3) using RI-ADC(2) level of theory. The results revealed that the PT in all clusters is complete within 84 fs, which was slower than that of 7AI$(H_2O)_{1,2}$ cluster. The difference in the ESPT time of 7AI$(H_2O)_n$ and 7AI$(MeOH)_n$ is reasonable because methanol is less polar than water.

Here, we simulated the PT dynamics of the 7AI$(H_2O)_2$, 7AI(MeOH–H_2O), and 7AI(H_2O–MeOH) complexes. Together with our previous data for 7AI$(MeOH)_2$ [20], we aim at systematically accessing the role of different solvents surrounding 7AI, the effect of mixing solvents, and the influence of different connections at the proton donor site (pyrrole moiety). Starting from a complex with two waters, the substitution of each water molecule by a methanol molecule should be very informative on PT dynamics in term of reaction probability and time constants.

2. Computational calculations

2.1. Static calculations

Ground-state optimizations of 7AI with water and mixed-solvent molecules, (a) 7AI$(H_2O)_2$, (b) 7AI(H_2O–MeOH), (c) 7AI(MeOH–H_2O) and (d) 7AI$(MeOH)_2$ complexes (Fig. 1) were calculated in the gas phase. The results for 7AI$(MeOH)_2$ have been reported before in Ref. [20]. These optimizations were done with the second-order algebraic diagrammatic construction method (ADC(2)) with the resolution-of-identity (RI) approximation for the electron-repulsion integrals [47,48], using the TURBOMOLE 5.10 program package [49,50]. The split valence polarized (SVP) basis set [51] was assigned to heavy atoms and hydrogen atoms involved in the hydrogen-bonded network, whereas the split valence (SV(P)) basis set was assigned to the remaining hydrogen atoms in the complexes. This level, hereafter referred as RI-ADC(2)/SVP-SV(P), is designed to keep the computational cost at an acceptable level, but still providing the accurate simulation results [20]. The minimum character of all optimized structures of 7AI with solvent clusters was confirmed by normal mode analysis. These optimized structures were further used for generating the initial conditions for excited-state dynamics simulations.

2.2. Excited-state dynamics simulation

Born–Oppenheimer dynamics simulations were carried out for 7AI$(H_2O)_2$, 7AI(H_2O–MeOH), 7AI(MeOH–H_2O) and 7AI$(MeOH)_2$ complexes in the first-excited state (S_1) at the RI-ADC(2)/SVP-SV(P) level. The results for 7AI$(MeOH)_2$ have been reported before in Ref. [20]. The initial conditions were generated using a harmonic-oscillator Wigner distribution for each normal mode. Dynamics and initial conditions were performed with the NEWTON-X program package [52,53] interfaced with TURBOMOLE. Twenty-five trajectories for each complex were simulated using a time step of 1 fs and maximum trajectory time of 300 fs. Statistical analysis was

Please cite this article in press as: R. Daengngern, et al., Dynamics simulations of excited-state triple proton transfer in 7-azaindole complexes with water, water–methanol and methanol, J. Photochem. Photobiol. A: Chem. (2013), http://dx.doi.org/10.1016/j.jphotochem.2013.05.012

Table 1
Summary of the ground-state structures computed at RI-ADC(2)/SVP-SV(P) level. Distances in Å, dihedral angles in degrees. $ø_1$ = N1C1N2C2, $ø_2$ = O1N1N2O2.

	Complex			
	7AI$(H_2O)_2$	7AI$(H_2O$–MeOH)	7AI(MeOH–H_2O)	7AI$(MeOH)_2$
R_1	1.739	1.738	1.731	1.730
R_2	1.716	1.714	1.698	1.698
R_3	1.822	1.796	1.817	1.789
N1—O1	2.775	2.773	2.766	2.765
O1—O2	2.680	2.680	2.662	2.662
O2—N2	2.803	2.771	2.798	2.767
$ø_1$	179.8	179.9	179.8	179.9
$ø_2$	−7.4	−9.8	−8.5	−11.8

Table 2
Summary of the excited-state dynamics performed at RI-ADC(2)/SVP-SV(P): number of trajectories following each of the three types of reactions (see text), ESPT probability, and average time to complete the first, second and third proton transfers (PT). Average distances at the PT time are given in parenthesis (in Å).

Complex	Reaction			ESPT probability	Time (fs)		
	ESPT ($\pi\pi^*$)	IC ($\pi\pi^*/S_0$)	No		PT1	PT2	PT3
7AI$(H_2O)_2$	9	2	14	0.36	50 (1.299)	55 (1.339)	58 (1.270)
7AI$(H_2O$–MeOH)	8	6	11	0.32	46 (1.328)	58 (1.290)	60 (1.311)
7AI(MeOH–H_2O)	11	1	13	0.44	71 (1.279)	83 (1.295)	85 (1.332)
7AI$(MeOH)_2$	16	4	5	0.64	68 (1.308)	81 (1.271)	84 (1.334)

carried out to provide information on average energies of each state, on internal coordinates, relative potential energy profiles and time evolution of the PT reactions along the hydrogen-bonded network. Average energy profiles were analyzed in terms of characteristic points along the reaction pathways, namely Normal (N), Intermediary Structure (IS), and Tautomer (T). N was chosen as the geometry at time zero. The IS1 point was assigned to the structure with the proton in the middle way between the pyrrole ring and the first solvent molecule. The IS2 point was assigned to the structure with a proton in the middle way between the two solvent molecules. The IS3 point was assigned to the structure with the proton in the middle way between the second solvent and the pyridine ring. The T point was selected right after last PT was completed. Furthermore, molecular orbitals of different electronic transitions were characterized for a representative trajectory of each complex.

3. Results and discussion

3.1. Ground-state structure

The ground-state structures of all complexes were optimized using RI-ADC(2)/SVP-SV(P) to study the effect of the surrounding homogeneous and inhomogeneous solvent. Intermolecular hydrogen bonds, other important bond distances and dihedral angles are summarized in Table 1 (see Fig. 1 for definitions).

The results show that there are three intermolecular hydrogen bonds in the cyclic network: first, R_1(O1···H1), the hydrogen bond between a proton donor on pyrrole ring and the nearest solvent molecule; second, R_2(O2···H2), between the solvent molecules; and third, R_3(N2···H3), between the second solvent molecule and the pyridine ring. The four complexes are not significantly different because of the structural similarity between water and methanol. Nevertheless, when a methanol molecule replaces a water molecule, the intermolecular hydrogen bonds become stronger, as evidenced by shorter hydrogen bonds. Even stronger hydrogen bonds are obtained with 7AI$(MeOH)_2$ complex, as shown in previous reports [20,29,31]. The optimized structure of 7AI is planar, as indicated by the dihedral angle $ø_1$ (N1C1N2C2) close to 180° for all complexes (Table 1). In addition, the hydrogen bonded network is also almost planar, as indicated by $ø_2$ (O1N1N2O2) absolute values smaller than 12°.

3.2. Excited-state dynamics simulations

The simulated trajectories for each complex were categorized into three types of reactions: (1) "ESPT" when a proton is completely transferred within simulation time; (2) "IC" when $S_1(\pi\pi^*)/S_0$ crossing is reached within simulation time; and (3) "No" (for "No Transfer") when a complete PT does not occur within the simulation time. The S_1/S_0 crossing in type 2 suggests that internal conversion should take place. This process will not, however, be investigated further in this work due to the limitations of the ADC(2), as a single-reference method, to deal with S_1/S_0 crossings. The number of trajectories following each type of reaction, the probability of PT, and average time of PT for each complex is summarized in Table 2. By definition, the transfer time from an atom X to an atom Y is taken as the time for which the X–H distance becomes equal to the H–Y distance [20]. This distance, averaged over all trajectories of type 1, is also given in Table 2.

To determine whether a hydrogen atom or a proton is transferred, the relative energy of the ground and excited states at the N, IS, and T points along hydrogen-bonded network for all complexes were computed for representative trajectories of type 1 (Figures S1–S4 of the Supplementary Data). For example, a potential energy diagram of the complete reaction for the 7AI$(H_2O)_2$ complex (Figure S1) shows that the $\pi\sigma^*$ lies over 70 kcal mol^{-1} above the $\pi\pi^*$ state for N, IS and T points. No crossing between these states was observed. This situation, which is the same for all trajectories, shows that dynamics takes place only on the $\pi\pi^*$ state, characterizing the transfer as a PT process.

3.2.1. 7AI$(H_2O)_2$ complex

From 25 trajectories of the 7AI$(H_2O)_2$ complex, 9 underwent excited-state triple proton transfer (ESTPT) reaction (type 1). Two trajectories achieved a region of degeneracy between $S_1(\pi\pi^*)$ and S_0 and could not be continued because of the limitation of the current method (type 2). The PT process did not take place in 14 trajectories during the simulation time (type 3). A back-PT reaction was also observed in some trajectories. Thus, the PT reaction probability is 36%.

Details of the PT process can be illustrated by analysis of a representative trajectory (Fig. 2). The atom numbering is the same as defined in Fig. 1(a). A normal (N) form is observed at time 0. The proton departs from the pyrrole ring to O1 atom of the nearest water

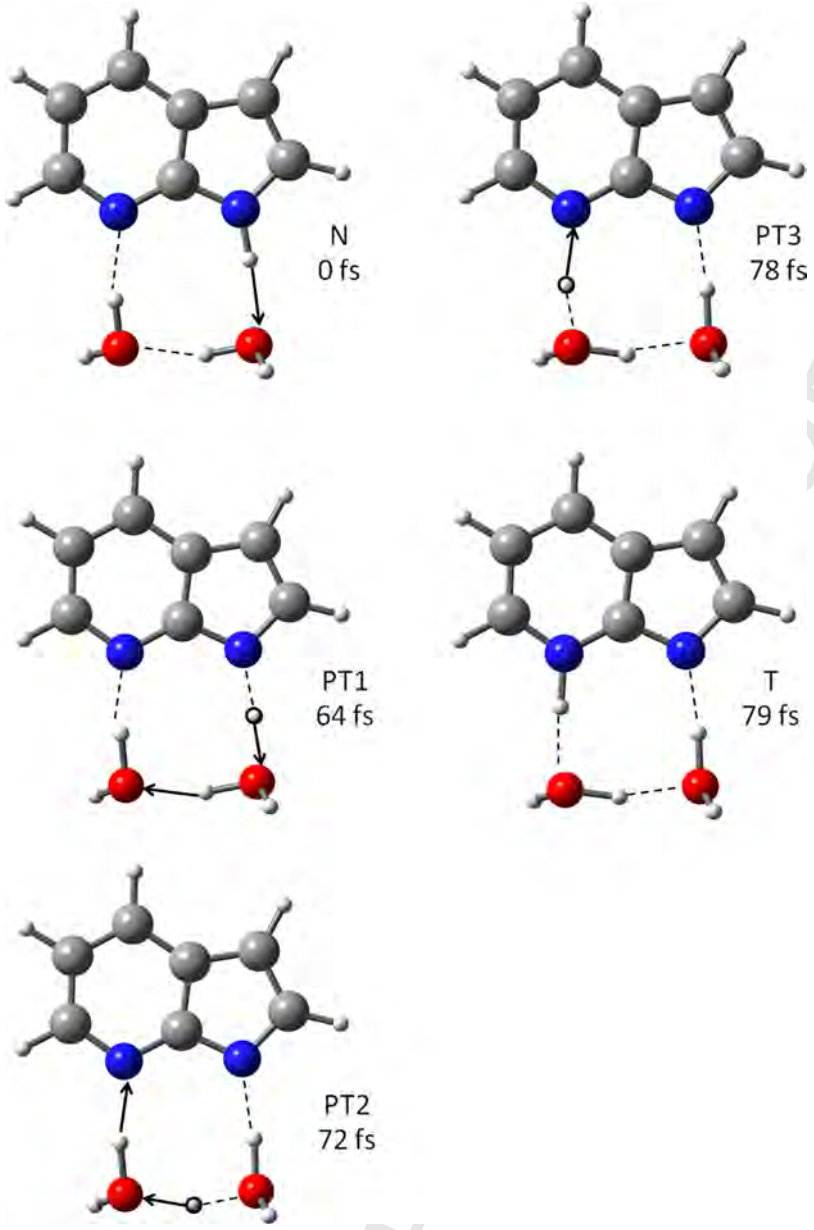

Fig. 2. Snapshots of a representative trajectory of the $7Al(H_2O)_2$ complex showing the time evolution of the ESTPT reaction through a hydrogen-bonded network within 79 fs. Averaged over all type-1 trajectories, this reaction is completed within 58 fs. Normal (N), proton transfer (PT), and tautomer (T).

(PT1) at 64 fs, and then a proton is transferred from this water to the second water (PT2) at 72 fs. Short afterwards, a proton of the second water moves to N2 in the pyridine ring (PT3) at 78 fs, and the tautomer (T) form is achieved within 79 fs. After completing the reaction, the complex dissociates.

Average values for geometric parameters and energies for the 9 trajectories following the ESTPT reaction are shown in Fig. 3 and 4, respectively. The evolution of the average values of three breaking bonds (N1—H1, O1—H2, and O2—H3) and three forming bonds (O1···H1, O2···H2 and N2···H3) is shown in Fig. 3(a). The intersection between the lines indicates that, on average, the first PT occurs at 50 fs when N1—H1 and O1—H1 bond lengths are equal to 1.299 Å, while the second PT occurs at 55 fs when O2—H3 and N2—H3 are equal to 1.339 Å, and the third PT occurs at 58 fs when O1—H2 and O2—H2 are equal to 1.270 Å (these values are compiled in Table 2). There is a certain time lag (~5 fs) between first and second PT, and a 3 fs time lag between the second PT and the third PT. These results characterize the process as asynchronous concerted triple PT.

It is noteworthy to compare our dynamics results with those for $7Al(H_2O)_2$ computed at state-specific CASSCF/DZP level reported by Kina et al. [40]. In that work, a single trajectory was computed with initial energy right above the threshold for PT. The ESTPT time was estimated to be 40–60 fs. The present result (58 fs) based on an average over an ensemble of trajectories is in close agreement with that of Ref. [40]. Fig. 4 shows that the average energy difference between $S_1(\pi\pi^*)$ and S_0 gradually decreases in the first 100 fs. After that, the average energy difference is above 40 kcal mol^{-1}, reflecting the structural planarity of the complex in the next 200 fs. This feature diverges from the dynamics results from Ref. [40]. There, the energy difference during the dynamics was about 20 kcal mol^{-1}, with ring-puckering oscillations bringing 7AI near a conical intersection. This result was interpreted as an indication that internal conversion could take place after the PT. Nevertheless, complementary calculations for the tautomer at the state averaged CASSCF and CASPT2 levels, also reported in Ref. [40], indicated rather larger energy differences (about 48 and

Please cite this article in press as: R. Daengngern, et al., Dynamics simulations of excited-state triple proton transfer in 7-azaindole complexes with water, water–methanol and methanol, J. Photochem. Photobiol. A: Chem. (2013), http://dx.doi.org/10.1016/j.jphotochem.2013.05.012

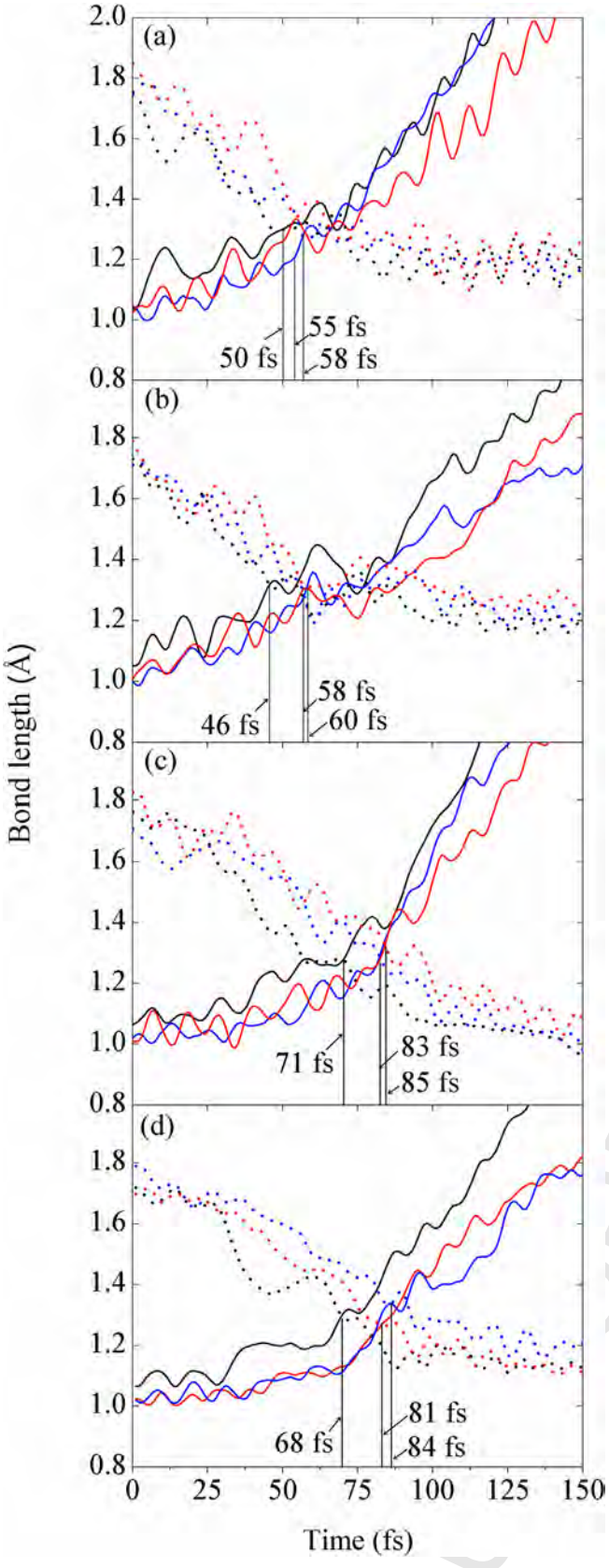

Fig. 3. Average breaking and forming bonds showing time evolution (PT time): (a) average value over 9 trajectories of the 7Al(H_2O)$_2$ complex, (b) average values over 8 trajectories of the 7Al(H_2O–MeOH) complex, (c) average values over 11 trajectories of the 7Al(MeOH–H_2O) complex, and (d) average value over 16 trajectories of the 7Al(MeOH)$_2$ complex. N1—H1 and O1···H1 in black, O1—H2 and O2···H2 in blue, and O2—H3 and N2···H3 in red. (For interpretation of the references to color in this figure legend, the reader is referred to the web version of this article.)

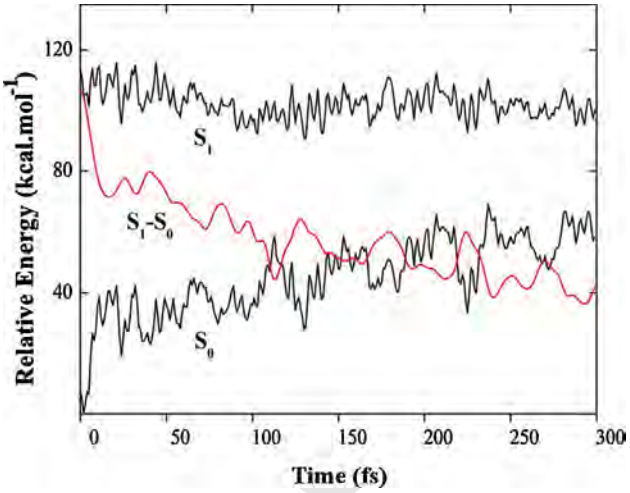

Fig. 4. Average potential energy diagram of complete reaction trajectories for 7Al(H_2O)$_2$ complex in the ground state (S_0) and excited states ($\pi\pi^*$, $\pi\sigma^*$) performed at RI-ADC(2)/SVP-SV(P) level.

54 kcal mol^{-1}, respectively), which are closer to the present results. We cannot discard, however, the possibility of later internal conversion, because at the end of our simulations at 300 fs, the average energy difference was still not in the equilibrium regime (Fig. 4).

3.2.2. 7Al(H_2O–MeOH) complex

The ESTPT reaction occurred in 8 out of 25 trajectories, while no reaction was observed in 11 trajectories and 6 trajectories reached a region of degeneracy between $S_1(\pi\pi^*)$ and S_0. Therefore, the PT probability is 32%, slightly smaller than that for the 7Al(H_2O)$_2$ complex (see Table 2). A representative trajectory (Fig. 5) illustrates how ESTPT reaction takes place. Starting from normal form (N), the process is summarized in the following three steps (the atom numbering is the same as defined in Fig. 1(b)): (1) a proton departs from N1 on pyrrole ring to O1 of the nearest water molecule (PT1) at 64 fs; (2) a proton moves from O1 of water to O2 of methanol (PT2) at 76 fs; and (3) a proton leaves O2 of methanol toward N2 on the pyridine ring (PT3) at 80 fs. For this trajectory, the complete ESPT reaction is obtained after 82 fs and followed by the complex dissociation.

The average values over 8 trajectories of the three breaking bonds (N1—H1, O1—H2, and O2—H3) increase, at the same time, the average values of the forming bonds (O1···H1, O2···H2 and N2···H3) decrease, as shown in Fig. 3(b). The first PT process occurs at 46 fs when the average N1—H1 and H1—O1 distances are equal to 1.328 Å (Table 2). The second proton transfers from water to methanol at 58 fs when the average O1—H2 and O2—H2 distances are equal to 1.290 Å. This leads to a certain time lag (~12 fs) between the first PT and second PT. The last PT occurs at 60 fs when the average O2—H3 and N2—H3 distances are equal to 1.311 Å. This dynamics behavior indicates an asynchronous concerted process.

3.2.3. 7Al(MeOH–H_2O) complex

For the 7Al(MeOH–H_2O) complex, 11 trajectories exhibited the ESTPT reaction, while 13 trajectories exhibited no reaction within the simulation time. Only one trajectory proceeded through $S_1(\pi\pi^*)/S_0$ crossing. Thus, the PT reaction probability is 44% (Table 2). A representative trajectory (Fig. 6) shows the ESTPT reaction as the proton moves along the hydrogen-bonded network. For this trajectory, the first, second, and third PT processes occur at 53, 69, and 81 fs, respectively, until the tautomer (T) is formed at 83 fs.

The atom numbering is the same as defined in Fig. 1(c). With the same criteria used in the 7Al(H_2O)$_2$ and 7Al(H_2O–MeOH) complexes, we found that for 7Al(MeOH–H_2O) the average times are

Please cite this article in press as: R. Daengngern, et al., Dynamics simulations of excited-state triple proton transfer in 7-azaindole complexes with water, water–methanol and methanol, J. Photochem. Photobiol. A: Chem. (2013), http://dx.doi.org/10.1016/j.jphotochem.2013.05.012

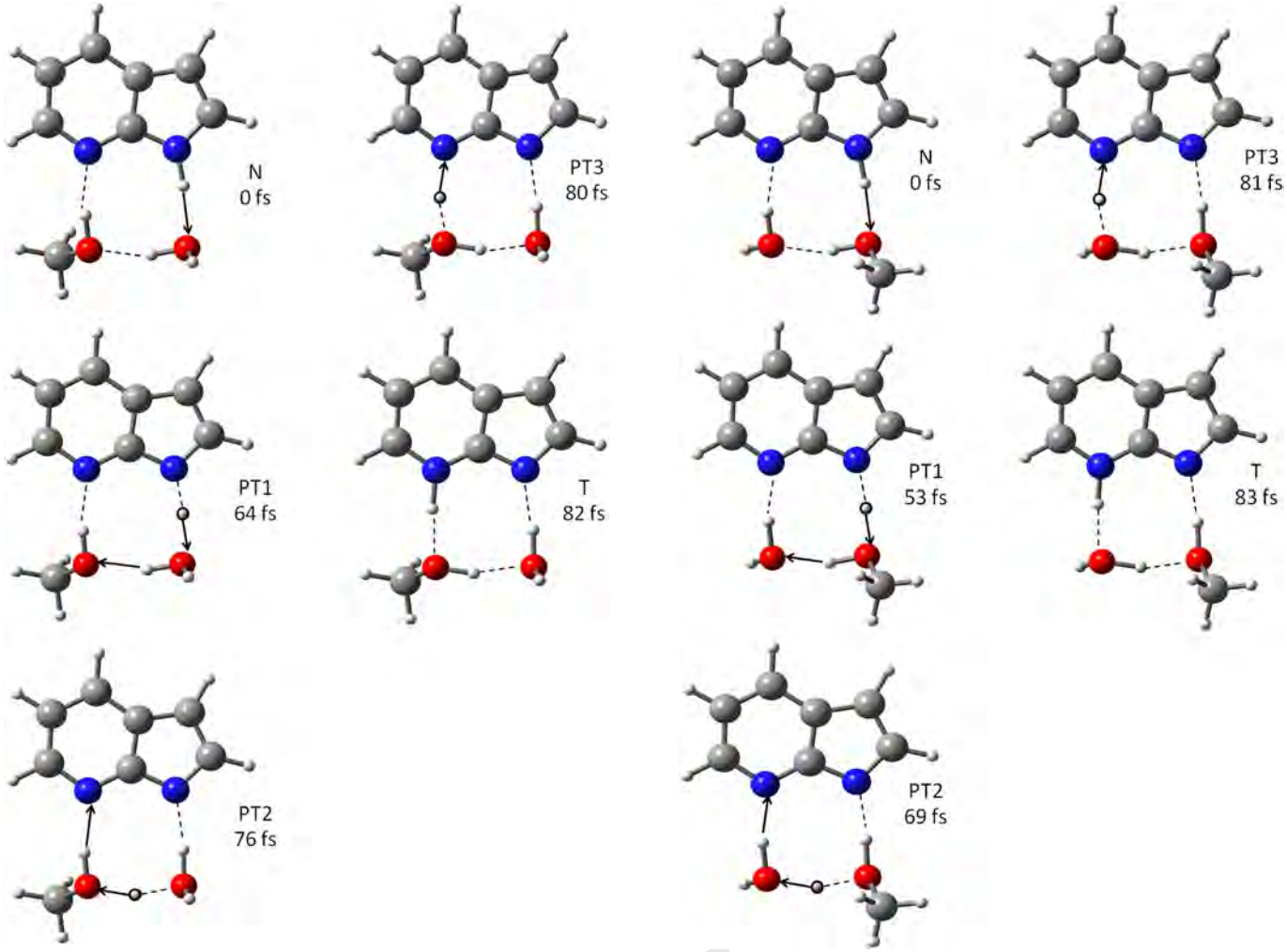

Fig. 5. Snapshots from a representative trajectory of the 7AI(H_2O–MeOH) complex, showing the time evolution of the ESTPT reaction through a hydrogen-bonded network within 82 fs. Averaged over all type-1 trajectories, this reaction is completed within 60 fs.

Fig. 6. Snapshots for a representative trajectory of the 7AI(MeOH–H_2O) complex showing the time evolution of the ESTPT reaction through a hydrogen-bonded network within 83 fs. Averaged over all type-1 trajectories, this reaction is completed within 85 fs.

71, 83, and 85 fs with bond distances of 1.279 Å (N1—H1=O1—H1), 1.295 Å (O1—H2=O2—H2), and 1.332 Å (O2—H3=N2—H3), respectively (see Fig. 3(c) and Table 2). There is a certain time lag (~12 fs) between the first PT and second PT, but time lags between the second PT and third PT is only 2 fs implying that the asynchronous concerted mechanism is also favorable for this complex.

3.2.4. 7AI(MeOH)$_2$ complex

In Ref. [20], we have reported dynamics results for 7AI(MeOH)$_n$ (n = 1–3) computed also at the RI-ADC(2)/SVP-SV(P) level used in this work. In this section, we summarize the data for 7AI(MeOH)$_2$ for a sake of completeness of the series of complexes investigated here. The ESTPT reactions occurred in 16 trajectories, while 5 trajectories showed no reaction within the simulation time and 4 trajectories reached a region of degeneracy of $S_1(\pi\pi^*)/S_0$. Therefore, the probability is 64%, which is the highest among all investigated complexes (Table 2).

Using the atom numbering defined in Fig. 1(d) and with the same criteria in other complexes, we found that for 7AI(MeOH)$_2$ the average times for the first, second and third PT are 68, 81, and 84 fs with bond distances 1.308 Å, 1.271 Å, and 1.334 Å, respectively (see Fig. 3(d) and Table 2). There is a certain time lag (~13 fs) between the first PT and second PT, but the time lag between the second PT and third PT is only 3 fs indicating that the asynchronous concerted mechanism is also favorable for this complex.

3.3. Time and barrier height for proton transfer

For all trajectories of type 1 (complete ESTPT) of each complex, we computed the average energies of the ground (S_0) and the first-excited ($\pi\pi^*$) states for the normal (N), intermediary (IS1, IS2, and IS3), and tautomer (T) structures along the reaction pathway. They are shown in Table 3 and Fig. 7.

The results in Table 3 and Fig. 7 show that the average excited-state reaction path has barriers of 3, 6, 2, and 2 kcal mol^{-1} for the 7AI(H_2O)$_2$, 7AI(H_2O–MeOH), 7AI(MeOH–H_2O), and 7AI(MeOH)$_2$, respectively. The average excited-state barriers nicely correlate with the PT probability reported in Table 2. In particular, it helps to rationalize why the probability of the PT reaction increases from 32% to 44% in the comparison between 7AI(H_2O–MeOH) and 7AI(MeOH–H_2O). Additionally, the larger excited-state barrier for 7AI(H_2O)$_2$ than for 7AI(MeOH)$_2$ is in good agreement with results reported by Fang et al. [22,23] using MRPT2/CASSCF method.

The excited-state barrier for tautomerization in 7AI is dramatically decreased when assisted with solvents (water or methanol) [22,23,41,54]. These solvent molecules play an important role in

Please cite this article in press as: R. Daengngern, et al., Dynamics simulations of excited-state triple proton transfer in 7-azaindole complexes with water, water–methanol and methanol, J. Photochem. Photobiol. A: Chem. (2013), http://dx.doi.org/10.1016/j.jphotochem.2013.05.012

Table 3
Average relative ground (S_0) and excited states ($\pi\pi^*$) energies (kcal mol^{-1}) of all type 1 trajectories for each complex for characteristic points.

State	Form	Complex			
		7AI(H_2O)$_2$	7AI(H_2O–MeOH)	7AI(MeOH–H_2O)	7AI(MeOH)$_2$
S_0	NIS1IS2IS3T	0 36 37 35 30	0 37 45 46 38	0 32 35 37 26	0 36 38 40 26
S_1 ($\pi\pi^*$)	NIS1IS2IS3T	10410710310398	104110106105101	101 103 99 96 88	10310510410089

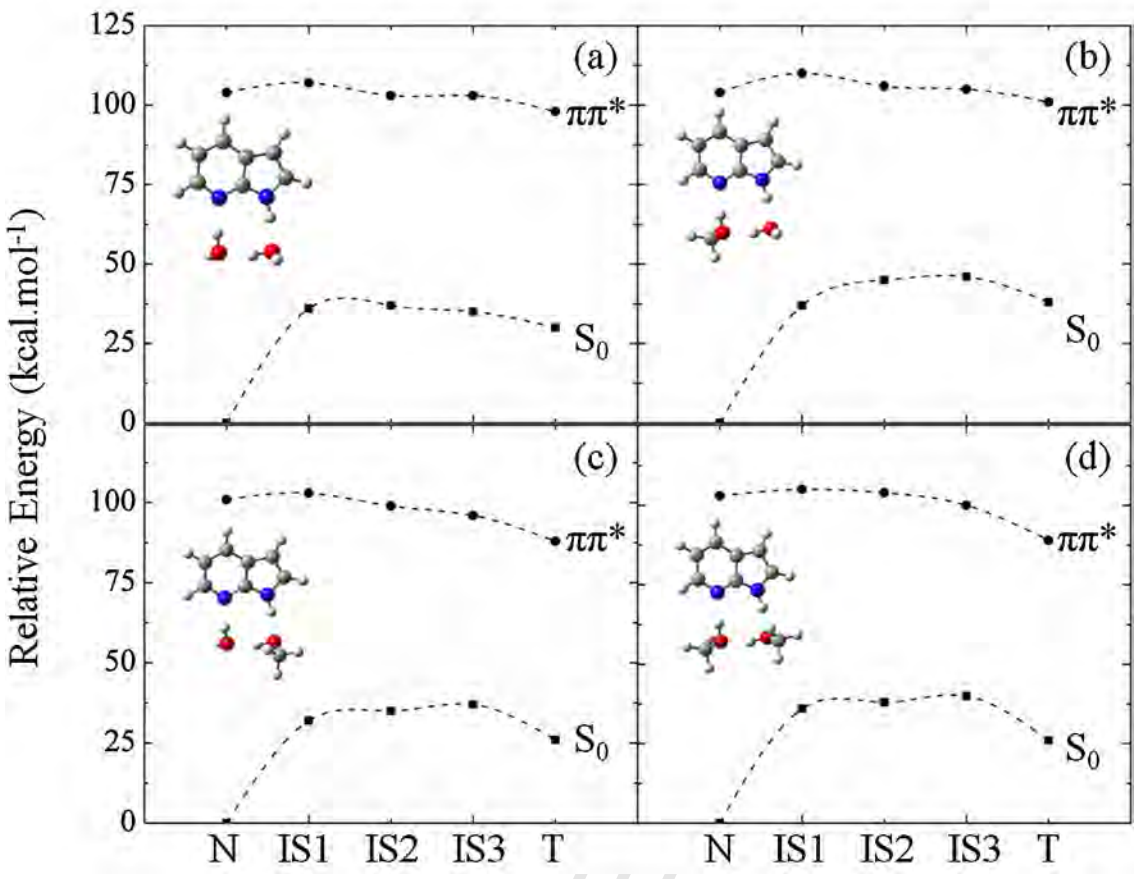

Fig. 7. Average relative energies (kcal mol^{-1}) of the ground (S_0) and the excited states ($\pi\pi^*$) of (a) 7AI(H_2O)$_2$, (b) 7AI(H_2O–MeOH), (c) 7AI(MeOH–H_2O), and (d) 7AI(MeOH)$_2$ complexes.

reducing the activation energy of tautomerization and also in stabilizing 7AI tautomer. The role played by the solvent effect is more pronounced when replacing water with methanol [22,23] or partially replacing water with methanol, as in this current work. When increasing number of methanol or replacing it in place of water in the site near the pyrrole, the intermolecular hydrogen bonds between 7AI and methanol become stronger due to the attractive force interaction between them. This effect can certainly shift the excited-state barrier and also the probability of the PT reaction.

ESTPT in 7AI(H_2O–MeOH) and 7AI(H_2O)$_2$ is completed within 45–60 fs, whereas, ESTPT in 7AI(MeOH–H_2O) and 7AI(MeOH)$_2$ is completed within a slightly longer time, 70–85 fs. Our results show that methanol lowers the reaction barrier, increasing the PT probability. For the mixed water–methanol complexes, we have observed that if the water is positioned near the pyrrole moiety, dynamics results are similar to the results for the 7AI(H_2O)$_2$ complex. If, however, methanol is positioned near the pyrrole moiety, the results are similar to the results for 7AI(MeOH)$_2$. This implies that the first PT, from the pyrrole to the solvent molecule, is the rate determining step of the ESTPT reaction in these complexes.

Born–Oppenheimer dynamics simulations of light particles like protons may be subject to artifacts, especially because of the lack of quantum interference, neglecting of tunneling and missing nonadiabatic effects. As we discussed above, in the case of micro-solvated 7AI, the proton transfer occurs barrierless or with small barriers after the photoexcitation and there are no state crossing along the reaction pathway. When these two conditions are satisfied, all three quantum effects listed above are minimized and the proton transfer behaves as a ballistic process which can be treated classically. Moreover, our classical simulations have also been useful to detect the possibility of nonadiabatic effects occurring to a fraction of trajectories approaching the state crossing.

4. Conclusions

Excited-sate dynamics simulations were carried out for 7AI(H_2O)$_2$, 7AI(H_2O–MeOH), 7AI(MeOH–H_2O), and 7AI(MeOH)$_2$ complexes at RI-ADC(2)/SVP-SV(P) level. These simulations revealed that sub 100 fs excited-state proton transfer reactions may take place for all complexes.

Please cite this article in press as: R. Daengngern, et al., Dynamics simulations of excited-state triple proton transfer in 7-azaindole complexes with water, water–methanol and methanol, J. Photochem. Photobiol. A: Chem. (2013), http://dx.doi.org/10.1016/j.jphotochem.2013.05.012

The transfer process pathway is most likely a PT, suggested by no crossing between $\pi\pi^*$ and $\pi\sigma^*$ states for all complexes. The proton transfer probabilities are between 32 and 64% depending on the cluster. They are substantially larger when a MeOH is near the pyrrole ring than when a water molecule is there. Also PT times are slightly longer when MeOH is near the pyrrole ring. The average excited-state barriers of the first PT with clusters of 7AI having MeOH placed near pyrrole are lower than those clusters of 7AI having water near pyrrole. Thus, the PT from pyrrole position to the solvent molecule is most likely the rate determining step of the ESTPT reaction. This step plays an important role in characterization of the dynamics behavior such as time evolution and reaction probability. All ESTPT processes are completed within 85 fs and showed an asynchronous concerted mechanism, with a time lag lower than 15 fs regardless of the kind of solvent molecules.

Indication of internal conversion prior the proton transfer was observed in all clusters. No conclusive indication of internal conversion after the proton transfer was observed.

Acknowledgements

The authors wish to thank the Thailand Research Fund (MRG5480294 and RTA5380010) for financial support. They also would like to express grateful acknowledgment to the Department of Chemistry, Faculty of Science, Chiang Mai University. R. Daengngern and K. Kerdpol thank the Research Professional Development Project under the Science Achievement Scholarship of Thailand (SAST), Faculty of Science, Chiang Mai University, Chiang Mai, Thailand.

Appendix A. Supplementary data

Supplementary data associated with this article can be found, in the online version, at http://dx.doi.org/10.1016/j.jphotochem.2013.05.012.

References

[1] L.G. Arnaut, S.J. Formosinho, Excited-state proton transfer reactions. I. Fundamentals and intermolecular reactions, Journal of Photochemistry and Photobiology A 75 (1993) 1.
[2] S.J. Formosinho, L.G. Arnaut, Excited-state proton transfer reactions. II. Intramolecular reactions, Journal of Photochemistry and Photobiology A 75 (1993) 21.
[3] F.S. Rodembusch, F.P. Leusin, L.F. da Costa Medina, A. Brandelli, V. Stefani, Synthesis and spectroscopic characterisation of new ESIPT fluorescent protein probes, Photochemical & Photobiological Sciences 4 (2005) 254.
[4] T.-I. Kim, H.J. Kang, G. Han, S.J. Chung, Y. Kim, A highly selective fluorescent ESIPT probe for the dual specificity phosphatase MKP-6, Chemical Communications (Cambridge, UK) (2009) 5895.
[5] R. Morales Alma, J. Schafer-Hales Katherine, O. Yanez Ciceron, V. Bondar Mykhailo, V. Przhonska Olga, I. Marcus Adam, D. Belfield Kevin, Excited state intramolecular proton transfer and photophysics of a new fluorenyl two-photon fluorescent probe, Chemphyschem 10 (2009) 2073.
[6] P.T. Chou, S.L. Studer, M.L. Martinez, Practical and convenient 355-nm and 337-nm sharp-cut filters for multichannel Raman spectroscopy, Journal of Applied Spectroscopy 45 (1991) 513.
[7] S.M. Chang, Y.J. Tzeng, S.Y. Wu, K.Y. Li, K.L. Hsueh, Emission of white light from 2-(2′-hydroxyphenyl) benzothiazole in polymer electroluminescent devices, Thin Solid Films 477 (2005) 38.
[8] S.M. Chang, K.L. Hsueh, B.K. Huang, J.H. Wu, C.C. Liao, K.C. Lin, Solvent effect of excited state intramolecular proton transfer in 2-(2′-hydroxyphenyl) benzothiazole upon luminescent properties, Surface and Coatings Technology 200 (2006) 3278.
[9] J. Catalan, On the evidence obtained by exciting 7-azaindole at 320 nm in 10^{-2} M solutions. Reply, Journal of Physical Chemistry A 107 (2003) 5642.
[10] J. Catalan, On the molecular structure that produces the phosphorescence of 7-azaindole, International Journal of Quantum Chemistry 102 (2005) 489.
[11] J. Catalan, V.J.C. del, M. Kasha, Resolution of concerted versus sequential mechanisms in photo-induced double-proton transfer reaction in 7-azaindole H-bonded dimer, Proceedings of the National Academy of Sciences of the United States of America 96 (1999) 8338.
[12] J. Catalan, P. Perez, V.J.C. del, P.J.L.G. de, M. Kasha, H-bonded N-heterocyclic base-pair phototautomerizational potential barrier and mechanism: the 7-azaindole dimer, Proceedings of the National Academy of Sciences of the United States of America 101 (2004) 419.
[13] C.-P. Chang, H. Wen-Chi, K. Meng-Shin, P.-T. Chou, J.H. Clements, Acid catalysis of excited-state double-proton transfer in 7-azaindole, Journal of Physical Chemistry A 98 (1994) 8801.
[14] Y. Chen, F. Gai, J.W. Petrich, Solvation and excited-state proton transfer of 7-azaindole in alcohols, Chemical Physics Letters 222 (1994) 329.
[15] Y. Chen, R.L. Rich, F. Gai, J.W. Petrich, Fluorescent species of 7-azaindole and 7-azatryptophan in water, Journal of Physical Chemistry 97 (1993) 1770.
[16] P.T. Chou, M.L. Martinez, W.C. Cooper, S.T. Collins, D.P. McMorrow, M. Kasha, Monohydrate catalysis of excited-state double-proton transfer in 7-azaindole, Journal of Physical Chemistry 96 (1992) 5203.
[17] P.-T. Chou, C.-Y. Wei, C.-P. Chang, M.-S. Kuo, Structure and thermodynamics of 7-azaindole hydrogen-bonded complexes, Journal of Physical Chemistry 99 (1995) 11994.
[18] P.-T. Chou, C.-Y. Wei, G.-R. Wu, W.-S. Chen, Excited-state double proton transfer in 7-azaindole analogues: observation of molecular-based tuning proton-transfer tautomerism, Journal of the American Chemical Society 121 (1999) 12186.
[19] P.-T. Chou, W.-S. Yu, Y.-C. Chen, C.-Y. Wei, S.S. Martinez, Ground-state reverse double proton transfer of 7-azaindole, Journal of the American Chemical Society 120 (1998) 12927.
[20] R. Daengngern, N. Kungwan, P. Wolschann, A.J.A. Aquino, H. Lischka, M. Barbatti, Excited-state intermolecular proton transfer reactions of 7-azaindole$(MeOH)_n$ (n = 1–3) clusters in the gas phase: on-the-fly dynamics simulation, Journal of Physical Chemistry A 115 (2011) 14129.
[21] H. Fang, Y. Kim, Solvent effects in the excited-state tautomerization of 7-azaindole: a theoretical study, Journal of Physical Chemistry B 115 (2011) 15048.
[22] H. Fang, Y. Kim, Theoretical studies for excited-state tautomerization in the 7-azaindole-$(CH_3OH)_n$ (n = 1 and 2) complexes in the gas phase, Journal of Physical Chemistry A 115 (2011) 13743.
[23] H. Fang, Y. Kim, Excited-state tautomerization in the 7-azaindole-$(H_2O)_n$ (n = 1 and 2) complexes in the gas phase and in solution: a theoretical study, Journal of Chemical Theory and Computation 7 (2011) 642.
[24] D.E. Folmer, E.S. Wisniewski, S.M. Hurley, A.W. Castleman Jr., Femtosecond cluster studies of the solvated 7-azaindole excited state double-proton transfer, Proceedings of the National Academy of Sciences of the United States of America 96 (1999) 12980.
[25] D.E. Folmer, E.S. Wisniewski, J.R. Stairs, A.W. Castleman, Water-assisted proton transfer in the monomer of 7-azaindole†, Journal of Physical Chemistry A 104 (2000) 10545.
[26] W.-T. Hsieh, C.-C. Hsieh, C.-H. Lai, Y.-M. Cheng, M.-L. Ho, K.K. Wang, G.-H. Lee, P.-T. Chou, Excited-state double proton transfer in model base pairs: the stepwise reaction on the heterodimer of 7-azaindole analogues, Chemphyschem 9 (2008) 293.
[27] Y. Kageura, K. Sakota, H. Sekiya, Charge transfer interaction of intermolecular hydrogen bonds in 7-azaindole$(MeOH)_n$ (n = 1, 2) with IR-Dip spectroscopy and natural bond orbital analysis, Journal of Physical Chemistry A 113 (2009) 6880.
[28] O.-H. Kwon, A.H. Zewail, Double proton transfer dynamics of model DNA base pairs in the condensed phase, Proceedings of the National Academy of Sciences of the United States of America 104 (2007) 8703.
[29] K. Sakota, N. Inoue, Y. Komoto, H. Sekiya, Cooperative triple-proton/hydrogen atom relay in 7-azaindole$(CH_3OH)_2$ in the gas phase: remarkable change in the reaction mechanism from vibrational-mode specific to statistical fashion with increasing internal energy, Journal of Physical Chemistry A 111 (2007) 4596.
[30] K. Sakota, C. Jouvet, C. Dedonder, M. Fujii, H. Sekiya, Excited state triple-proton transfer in 7-azaindole$(H_2O)_2$ and reaction path studied, Journal of Physical Chemistry A 114 (2010) 11161.
[31] K. Sakota, Y. Kageura, H. Sekiya, Cooperativity of hydrogen-bonded networks in 7-azaindole$(CH_3OH)_n$ (n = 2, 3) clusters evidenced by IR-UV ion-dip spectroscopy and natural bond orbital analysis, Journal of Chemical Physics 129 (2008), 054303/1.
[32] K. Sakota, Y. Komoto, M. Nakagaki, W. Ishikawa, H. Sekiya, Observation of a catalytic proton/hydrogen atom relay in microsolvated 7-azaindole-methanol cluster enhanced by a cooperative motion of the hydrogen-bonded network, Chemical Physics Letters 435 (2007) 1.
[33] K. Sakota, N. Komure, W. Ishikawa, H. Sekiya, Spectroscopic study on the structural isomers of 7-azaindole$(ethanol)_n$ (n = 1–3) and multiple-proton transfer reactions in the gas phase, Journal of Chemical Physics 130 (2009), 224307/1.
[34] A.S. Smirnov, D.S. English, R.L. Rich, J. Lane, L. Teyton, A.W. Schwabacher, S. Luo, R.W. Thornburg, J.W. Petrich, Photophysics and biological applications of 7-azaindole and its analogs, Journal of Physical Chemistry B 101 (1997) 2758.
[35] C.A. Taylor, M.A. El-Bayoumi, M. Kasha, Excited-state two-proton tautomerism in hydrogen-bonded N-heterocyclic base pairs, Proceedings of the National Academy of Sciences of the United States of America 63 (1969) 253.
[36] S.-B. Zhao, S. Wang, Luminescence and reactivity of 7-azaindole derivatives and complexes, Chemical Society Reviews 39 (2010) 3142.
[37] A.H. Zewail, Femtochemistry. Past, present, and future, Pure and Applied Chemistry 72 (2000) 2219.
[38] M.P.T. Duong, Y. Kim, Theoretical studies for the rates and kinetic isotope effects of the excited-state double proton transfer in the 1:1 7-azaindole:H_2O complex using variational transition state theory including multidimensional tunneling, Journal of Physical Chemistry A 114 (2010) 3403.

[39] M.P.T. Duong, K. Park, Y. Kim, Excited state double proton transfer of a 1:1 7-azaindole:H_2O complex and the breakdown of the rule of the geometric mean: variational transition state theory studies including multidimensional tunneling, Journal of Photochemistry and Photobiology A 214 (2010) 100.
[40] D. Kina, A. Nakayama, T. Noro, T. Taketsugu, M.S. Gordon, Ab initio QM/MM molecular dynamics study on the excited-state hydrogen transfer of 7-azaindole in water solution, Journal of Physical Chemistry A 112 (2008) 9675.
[41] G.M. Chaban, M.S. Gordon, The ground and excited state hydrogen transfer potential energy surface in 7-azaindole, Journal of Physical Chemistry A 103 (1999) 185.
[42] R.S. Moog, M. Maroncelli, 7-Azaindole in alcohols: solvation dynamics and proton transfer, Journal of Physical Chemistry 95 (1991) 10359.
[43] M.N.R. Ashfold, B. Cronin, A.L. Devine, R.N. Dixon, M.G.D. Nix, The role of $\pi\sigma^*$ excited states in the photodissociation of heteroaromatic molecules, Science (Washington, DC, United States) 312 (2006) 1637.
[44] C. Tanner, C. Manca, S. Leutwyler, Probing the threshold to H atom transfer along a hydrogen-bonded ammonia wire, Science (Washington, DC, United States) 302 (2003) 1736.
[45] C. Tanner, C. Manca, S. Leutwyler, Exploring excited-state hydrogen atom transfer along an ammonia wire cluster: competitive reaction paths and vibrational mode selectivity, Journal of Chemical Physics 122 (2005), 204326/1.
[46] C. Tanner, M. Thut, A. Steinlin, C. Manca, S. Leutwyler, Excited-state hydrogen-atom transfer along solvent wires: water molecules stop the transfer, Journal of Physical Chemistry A 110 (2006) 1758.
[47] C. Hättig, Geometry optimizations with the coupled-cluster model CC2 using the resolution-of-the-identity approximation, Journal of Chemical Physics 118 (2003) 7751.
[48] C. Hättig, Structure optimizations for excited states with correlated second-order methods: CC2 and ADC(2), Advances in Quantum Chemistry 50 (2005) 37.
[49] R. Ahlrichs, M. Bär, M. Häser, H. Horn, C. Kölmel, Electronic structure calculations on workstation computers: the program system TURBOMOLE, Chemical Physics Letters 162 (1989) 165.
[50] R. Ahlrichs, M. Bär, M. Häser, C. Kölmel, J. Sauer, Nonempirical direct SCF calculations on sodalite and double six-ring models of silica and aluminum phosphate (AlPO4) minerals: $H_{24}Si_{24}O_{60}$, $H_{12}Si_{12}O_{30}$, $H_{12}A_{l6}P_6O_{30}$, Chemical Physics Letters 164 (1989) 199.
[51] A. Schäfer, H. Horn, R. Ahlrichs, Fully optimized contracted Gaussian basis sets for atoms lithium to krypton, Journal of Chemical Physics 97 (1992) 2571.
[52] M. Barbatti, G. Granucci, M. Persico, M. Ruckenbauer, M. Vazdar, M. Eckert-Maksić, H. Lischka, The on-the-fly surface-hopping program system Newton-X: application to ab initio simulation of the nonadiabatic photodynamics of benchmark systems, Journal of Photochemistry and Photobiology A 190 (2007) 228.
[53] M. Barbatti, G. Granucci, M. Ruckenbauer, F. Plasser, J. Pittner, M. Persico, H. Lischka, Newton-X: a package for Newtonian dynamics close to the crossing seam, version 1.1, 2011 www.newtonx.org
[54] M.S. Gordon, Hydrogen transfer in 7-azaindole, Journal of Physical Chemistry 100 (1996) 3974.

Please cite this article in press as: R. Daengngern, et al., Dynamics simulations of excited-state triple proton transfer in 7-azaindole complexes with water, water–methanol and methanol, J. Photochem. Photobiol. A: Chem. (2013), http://dx.doi.org/10.1016/j.jphotochem.2013.05.012

Theoretical Chemistry Accounts

Theoretical study on excited-state intermolecular proton transfer reactions of 1H-pyrrolo[3,2-h]quinoline with water and methanol

--Manuscript Draft--

Manuscript Number:	
Full Title:	Theoretical study on excited-state intermolecular proton transfer reactions of 1H-pyrrolo[3,2-h]quinoline with water and methanol
Article Type:	Regular Article
Keywords:	ADC(2) dynamics simulation; Excited-state proton transfer (ESPT); Excited-state tautomerization; Solvent-assisted proton transfer; 1H-Pyrrolo[3,2-h]quinoline.
Corresponding Author:	Nawee Kungwan, Ph.D. Chiang Mai University Muang, Chiang Mai THAILAND
Corresponding Author Secondary Information:	
Corresponding Author's Institution:	Chiang Mai University
Corresponding Author's Secondary Institution:	
First Author:	Nawee Kungwan, Ph.D.
First Author Secondary Information:	
Order of Authors:	Nawee Kungwan, Ph.D.
	Rathawat Daengngern, Ph.D, Student
	Tammarat Piansawan, Master Student
	Supa Hannongbua, Ph.D.
	Mario Barbatti, Ph.D.
Order of Authors Secondary Information:	
Abstract:	The dynamics of ultrafast excited-state multiple intermolecular proton transfer (PT) reactions in complexes of 1H-pyrrolo[3,2-h]quinoline with water and methanol (PQ(H2O)n and PQ(MeOH)n, where n = 1, 2) is modeled using quantum-chemical simulations. The minimum energy ground-state structures of the complexes are determined. Molecular dynamics simulations in the first excited state are employed to determine reaction mechanisms and the time evolution of the PT processes. Excited-state dynamics results for all complexes reveal synchronous excited-state multiple proton transfer (ESmultiPT) via solvent-assisted mechanisms along an intermolecular hydrogen-bonded network. In particular, excited-state double proton transfer (ESDPT) is the most effective, occurring with the highest probability in the PQ(MeOH) cluster. The PT character of the reactions is suggested by nonexistence of crossings between ππ*and πσ* states.
Suggested Reviewers:	Masanori Tachikawa, Ph.D. Professor, Yokohama City University tachi@yokohama-cu.ac.jp
	Felix Plasser, Ph.D. University of Heidelberg felix.plasser@iwr.uni-heidelberg.de
	Hiroki Nakamura, Ph.D. Dinstinguished Consultant and Professor Emeritus, Institute for Molecular Science, Okazaki, Japan nakamura-1624@kba.biglobe.ne.jp
	Yongho Kim, Ph.D.

	Professor, Kyung Kee University ykkim@khu.ac.kr
	Michał F. Rode, Ph.D. Professor, Polish Academy of Sciences mrode@ifpan.edu.pl

Theoretical study on excited-state intermolecular proton transfer reactions of 1*H*-pyrrolo[3,2-*h*]quinoline with water and methanol

Nawee Kungwan,[*a] Rathawat Daengngern,[a] Tammarat Piansawan,[a] Supa Hannongbua,[b] and Mario Barbatti [c]

Department of Chemistry, Faculty of Science, Chiang Mai University, Chiang Mai 50200, Thailand

Department of Chemistry, Faculty of Science, Kasetsart University, Bangkhen Campus, Bangkok 10903, Thailand

Max-Planck-Institut für Kohlenforschung, Kaiser-Wilhelm-Platz 1, D-45470, Mülheim an der Ruhr, Germany

[*]Corresponding author. E-mail: naweekung@gmail.com.

Phone: +66-53-943341 ext 101. Fax: +66-53-892277.

[a] Department of Chemistry, Chiang Mai University.

[b] Department of Chemistry, Kasetsart University.

[c] Max-Planck-Institut für Kohlenforschung.

Abstract

The dynamics of ultrafast excited-state multiple intermolecular proton transfer (PT) reactions in complexes of 1*H*-pyrrolo[3,2-*h*]quinoline with water and methanol ($PQ(H_2O)_n$ and $PQ(MeOH)_n$, where n = 1, 2) is modeled using quantum-chemical simulations. The minimum energy ground-state structures of the complexes are determined. Molecular dynamics simulations in the first excited state are employed to determine reaction mechanisms and the time evolution of the PT processes. Excited-state dynamics results for all complexes reveal synchronous excited-state multiple proton transfer (ESmultiPT) via solvent-assisted mechanisms along an intermolecular hydrogen-bonded network. In particular, excited-state double proton transfer (ESDPT) is the most effective, occurring with the highest probability in the PQ(MeOH) cluster. The PT character of the reactions is suggested by nonexistence of crossings between ππ*and πσ* states.

Keywords: ADC(2) dynamics simulation, Excited-state proton transfer (ESPT), Excited-state tautomerization, Solvent-assisted proton transfer, 1*H*-Pyrrolo[3,2-*h*]quinoline .

1. Introduction

The proton transfer (PT) is one of the most important classes of chemical reactions [1-2]. Because PT processes often take place within hydrogen-bonded systems, and because of the central role played by hydrogen bonds in chemistry and biology, a large number of studies have been performed on PT processes in both the ground and excited states [3-4]. A special class of compounds exhibiting PT is represented by heteroaromatic molecules [5-7]. In particular, heteroazaaromatic or bifunctional molecules having a hydrogen-bonding donor group (e.g., a pyrrole NH) and a hydrogen-bonding acceptor group (e.g., a quinoline-type N) are of great interests for their dual photochromic properties in a variety of solvents. Examples of molecules exhibiting intramolecular PT are salicylic acid and its derivatives [8]. Naturally, intramolecular PT will occur preferentially when the spatial separation between the donor and the acceptor sites is small [9-10]. In the case of a larger separation, the PT should proceed through a hydrogen-bond bridge established within a protic solvent. The phenomenon of phototautomerization is driven by a PT process in which the process may occur either in an intramolecular [11-14] or an intermolecular [5-7,9-10,15-17] manners. Thus, hydrogen bonding networks of these molecules with the solvent must be formed before molecules undergo excited-state proton transfer (ESPT). The heteroazaaromatic molecule requires a catalytic transfer via a one-molecule hydrogen-bonded proton-donor-acceptor bridge, or a two or more molecule PT relay [18]. There are many compounds belonging to the class of *N*-heteroazaaromatic molecules which undergo intermolecular PT. Those most studied are 7-azaindole (7AI) [5-7,9,15-17,19-20], 7-hydroxyquinoline (7HQ) [21-23], and 1-*H*-pyrrolo[3,2-*h*]quinoline (PQ or pyrido[3,2-*g*]indole) [7,24-28], For a general review on this topic see refs [7,29].

The structure of PQ can be viewed as similar to that of 7AI, modified by the addition of a benzo-ring spacer, separating the pyrido and the pyrrolo rings. Potentially valuable applications of PQ and its derivatives for chemical and biomedical uses have been reported [25-27,30-31]. For example, PQ was proposed as a host molecule in molecular recognition and as a potential anticancer drug [32]. It also exhibited bioactivity against tuberculosis and malaria [8]. In chemical applications, 1-methyl-pyrrolo[3,2]quinolone was found to be a good stabilizer for polymers [18]. Moreover, dipyridol[2,3-*a*:3□,2□-*i*]carbazole (DPC) has been considered as a probe of hydrophilic/hydrophobic surface character [33]. To exhibit the photochemical activity necessary as a probe, PQ and its derivative must form hydrogen bonds with protic solvent partners.

Obviously, the geometry of PQ (Fig. 1) favors an internal hydrogen bond between the pyrrole NH and the pyridine N atom. PQ can, however, instead form a hydrogen-bonded network with solvent partners, especially water

and alcohols. Different stoichiometries of hydrogen-bonded complexes of PQ with water and methanol have been reported based on molecular dynamics simulations and density functional theory (DFT) [30,34]. 1:1 (doubly hydrogen-bonded) and 1:2 (triply hydrogen-bonded) cyclic complexes have been predicted to exist at low solvent concentrations and such complexes also existed in bulk solvent [34]. Both cyclic and non-cyclic hydrogen-bonded complexes have been determined. For $PQ(MeOH)_2$ complexes, DFT studies have shown that cyclic hydrogen-bonded species are more stable than non-cyclic ones. For PQ complexed with bulk water, the population of the 1:1 cyclic complex was found to be 3.5 times smaller than that of the cyclic complex in bulk methanol. A 1:2 complex, in which two water molecules form a cyclic hydrogen bonding network connecting the pyrrole N-H and the pyridine N atoms, has also been reported in studies combining infrared/femtosecond multiphoton ionization (IR/fsMPI) with fluorescence-detected infrared (FDIR) spectrometry associated with DFT calculations [24,27]. In such a cyclic hydrogen-bonded complex, triple PT through water bridges is possible upon excitation. The photophysics of jet-isolated complexes of PQ with water [27] and methanol [26] depends strongly on the cluster size. Complete lack of fluorescence was observed for the 1:1 complex, which has been justified by a fast ESPT reaction. Competing tautomerization as a result of the 1:2 complex might also contribute to the lack of fluorescence. The PT mechanism has previously been investigated by static calculations on the PQ with water and methanol complexes [26-27]. To the best of our knowledge, there are no previous reports on the dynamics of PT in the excited-state. Thus, to provide a more complete picture of ESPT in PQ-solvent complexes, dynamic simulations are required.

The aim of our work is to investigate the photoinduced tautomerization mechanism of PT reactions in cyclic hydrogen-bonded $PQ(H_2O)_n$ and $PQ(MeOH)_n$ (n = 1, 2) complexes in the lowest-excited singlet state. The methodology which we employ here, using the resolution-of-the-identity approximation for the electron repulsion integrals and algebraic diagrammatic construction through a second order method (RI-ADC(2)), was recently successfully applied by us to investigations of 7AI complexed with methanol molecules [9]. The goals of the present simulations are to determine the corresponding time constants of PT process and also the mechanistic pathways of PT in each complex. The probabilities of the ESPT processes in each of the complexes will be analyzed and compared. The PT character of the reactions will be also addressed in this work.

2. Computational Details

2.1 Ground-State Calculations

Ground-state optimizations of $PQ(H_2O)_{n=1,2}$ and $PQ(MeOH)_{n=1,2}$ complexes were performed in the gas phase using the RI-ADC(2) [35-36] and the SVP [37] basis set, implemented in the TURBOMOLE 5.10 program package [38]. The minimum energy characters of all optimized structures were confirmed by normal mode analysis. These optimized structures were also used in excited-state dynamics simulations as explained below.

2.2 Excited-State Dynamics Simulations

Molecular dynamics simulations were carried out for the $PQ(H_2O)_{n=1,2}$ and $PQ(MeOH)_{n=1,2}$ complexes on the energy surface of the first excited state (S_1). The initial conditions were generated using a harmonic-oscillator Wigner distribution [39] for each normal mode, as implemented in the NEWTON-X program package [40-41] interfaced with the TURBOMOLE program. To reduce the computational cost, RI-ADC(2) with the SVP mixed SV(P) basis sets were employed. The SVP-SV(P) basis set is defined by assigning the split valence polarized SVP basis set to heavy atoms and hydrogen atoms involved in the hydrogen-bonded network of a complex, and using the split valence SV(P) basis set for the remaining hydrogen atoms. This small but sufficiently accurate mixed basis set has been tested and used in both static and dynamics calculations reported in our previous studies [9,14,42]. Fifty trajectories for each complex were simulated using a time step of 1 fs throughout the simulations, each of these having a total duration of 300 fs. Molecular orbital characterizations of the different electronic transitions were performed to verify the character of reactions. Furthermore, a statistical analysis was also carried out to give detailed properties (e.g. energies and internal coordinates), which were used to obtain time evolution of the transfer reactions along the hydrogen-bonded network.

3. Results and Discussion

3.1 Ground-State Structures

The optimized structures of PQ with water and methanol complexes, with important atoms belonging to intermolecular hydrogen-bonded networks numbered, are shown in Fig. 1. To understand the surrounding cooperative effect of water and methanol molecules on the hydrogen bonds of the complexes, the ground-state structures of $PQ(H_2O)_{n=1,2}$ and $PQ(MeOH)_{n=1,2}$ complexes with cyclic hydrogen-bonded network were optimized at the RI-ADC(2)/SVP-SV(P) level. The intermolecular hydrogen bonds (dashed lines) are characterized in TABLE 1.

3.1.1 $PQ(H_2O)_{n=1,2}$

When one water molecule is added to PQ, a cyclic hydrogen-bonded complex is formed (Fig. 1a). There are two intermolecular hydrogen bonds labeled as R_1(O1···H1), with a bond length of 1.814 Å, and R_2(N2···H2), with a bond distance of 1.866 Å. For two water molecules, there are three hydrogen bonds (Fig. 1b). The first one, between the oxygen atom of the first water and the hydrogen atom of the pyrrole ring (R_1(O1···H1)), has a bond length of 1.786 Å, slightly shorter than that of the equivalent bond in PQ(H_2O). The second hydrogen bond, formed between the hydrogen atom of the second water and the pyridine N atom (R_2(N2···H3)), has a bond length of 1.794 Å, also shorter than that in PQ(H_2O). The third hydrogen bond (R_3(O2···H2)) is formed between the two waters and it has a length of 1.750 Å.

3.1.2 PQ(MeOH)$_{n=1,2}$

When one methanol molecule is added to PQ, a cyclic hydrogen-bonded complex is formed similarly as in PQ(H_2O). The PQ(MeOH) complex with relevant labels is shown in Fig. 1c. There are two hydrogen bonds in this complex: first, between the oxygen atom from methanol and the hydrogen from the pyrrole group (1.794 Å); second, between the hydrogen atom of methanol and the pyridine N atom (1.820 Å). The present RI-ADC(2) value for R_1 is shorter than the R_1 value computed at the MP2 level [26] by 0.08 Å. Values of R_2 computed with RI-ADC(2) and MP2 agree within 0.01 Å.

Starting from the PQ(MeOH) complex, a second methanol can be added. A cyclic intermolecular hydrogen-bonded network is formed with three hydrogen bonds (Fig. 1d). The first one, between the oxygen atom and the hydrogen atom of the pyrrole ring (R_1(O1···H1)), has a bond length of 1.743 Å, which is slightly shorter than the equivalent bond in PQ(H_2O). The second hydrogen bond links the hydrogen atom of methanol to the pyridine N atom of PQ (R_2(N2···H3)) with a bond length of 1.755 Å. The third hydrogen bond, formed by the interaction between the two methanol molecules (R_3(O2···H2)), has a bond length of 1.720 Å. The present RI-ADC(2) values for R_1 and R_2 are in good agreement with the MP2 values reported in ref [26]. However, we calculate a value of R_3 shorter than that determined at the MP2 level by about 0.04 Å.

Generally, complexes of PQ with water and methanol form similar structures with hydrogen-bonded network. Either with water or methanol, the larger number of solvent molecules increases the strength of the hydrogen bonding network, as can be seen from the systematic shortening of R_1 and R_2 with the increase of the cluster size. However, the differences between them are governed by the methyl group of methanol. For the 1:2 complex of PQ, the water bridge gives a more planar hydrogen-bonded network than the methanol. The characteristic O1N1N2O2 dihedral angles in the

ground state are 20.3 and 33.4 degrees for the water and methanol complexes, respectively. The difference between these dihedral angles may be caused by the interaction between the methyl group of methanol and the PQ molecule.

3.2 Excited-State Dynamics Simulation

Fifty trajectories with different initial conditions were computed for each complex. Carrying simulation times out to 300 fs should reveal the entire mechanisms, including pre- and post-transfer processes. The trajectories for $PQ(H_2O)_{n=1,2}$ and $PQ(MeOH)_{n=1,2}$ complexes were analyzed and classified into three different types of reactions: (1) "ESPT", when a proton (or hydrogen) is transferred within the simulation time; (2) "IC", when an $S_1(\boldsymbol{\pi\pi}^*)/S_0$ crossing is reached within the simulation time suggesting that internal conversion should take place; and (3) "No transfer" (NT), when no proton transfer occurs within the simulation time. The number of trajectories following each type of reaction, the PT probability, and the average transfer time for each complex are summarized in TABLE 2.

The PT time is given as the time when the bond-breaking distance averaged over all trajectories exhibiting PT intersects the average bond-forming distance. This is the same definition that we have used in our previous investigations [9,14,42]. The proton transfer mechanism can be assigned as either synchronous, concerted or stepwise depending on the delay time between two consecutive PTs [43]. If the delay time is shorter than about 10−15 fs, which corresponds to a vibrational period of N−H and O−H stretching modes, the PTs are synchronous, otherwise they are either concerted (a single kinetic step) or stepwise (two distinct kinetic steps via a stable intermediate).

To determine whether an excited-state proton transfer (PT) and/or an excited-state hydrogen atom transfer (HT) takes place during the dynamics, the relative energies of the ground (S_0) and the two lowest excited states ($\pi\pi^*$ and $\pi\sigma^*$) were computed along characteristic points of one single selected trajectory for each complex. These characteristic points are the complex at time 0 (normal or N), the intermediary structure (IS1 and IS2), and the tautomer structure (T). The IS1 and IS2 point were taken as the geometry when the hydrogen is midway between the donor and the acceptor atoms: IS1 as midway between the pyrrole NH of PQ and water, and IS2 as midway between water and the pyridine N of PQ. The T point was selected right after the transfer process was complete. The energies for each of these points (relative to the N point) are given in TABLE S2 in the Supplementary Material. Note that energies given in this table were computed for a single selected trajectory; therefore, they should not be taken as true energy barriers occurring on the energy surface. They provide, however, a qualitative picture of the reaction. For $PQ(H_2O)$, these

values are shown in the potential-energy diagram of Fig. 2. Similar diagrams for the other complexes are given in the Supplementary Material (Fig. S1, S2 and S3).

The main molecular orbitals involved in the excited states are also shown for each geometry in Fig. 2. The molecular orbital near S_0 is doubly occupied in the ground state. Upon excitation, it donates an electron to one of the orbitals pictured near the excited states. For instance, for the Normal structure in Fig. 2, the first excited state corresponds to a $\pi\pi^*$ excitation, while the second excited state corresponds to a $\pi\sigma^*$ excitation. The π and the π^* orbitals are completely localized on PQ whereas the σ^* orbital is delocalized over PQ and the water molecule (Fig. 2). These features are independent of the geometry and also hold for the other complexes (see the Supplementary Material). The only exception is the σ^* orbital in $PQ(MeOH)_2$, which is mostly localized on the solvent molecules.

The relative energies of the $\pi\pi^*$ and $\pi\sigma^*$ states along the transfer pathway play an important role in determining the nature of the excited-state reaction, since PT should occur in the $\pi\pi^*$ state, whereas the HT should occur in the $\pi\sigma^*$ state [27,44-45]. The results for $PQ(H_2O)$ from Fig. 2 show that, first, there is no crossing between $\pi\sigma^*$ and $\pi\pi^*$ and that, second, $\pi\sigma^*$ lies well above $\pi\pi^*$. This implies that the dynamics along the first excited state takes place purely in the $\pi\pi^*$ state, characterizing a PT process. The same feature holds for the other three complexes, as shown in Fig. S1, S2 and S3 of the Supplementary Material.

3.2.1 $PQ(H_2O)$ complex

On-the-fly dynamics simulations were carried out for 50 trajectories of the $PQ(H_2O)$ complex. A total of 12 trajectories showed excited-state double proton transfer (ESDPT) (24% probability, TABLE 2). The PT process did not occur in 31 trajectories during the simulation time. Seven trajectories reached a small energy gap between S_1 and S_0 (< 0.5 eV) and could not be continued because of limitations of RI-ADC(2) in dealing with such multireference regions of the potential energy surface. Back-PT reaction was also observed in some trajectories. The structures along the reaction pathway are depicted in Fig. 3 for a selected trajectory. The PT process, indicated by an arrow, can be described by the following events: First, a normal (N) form is observed at time 0. Second, the first proton (H1) moves from N1 on the pyrrole ring to the O1 atom (PT1) at 72 fs, then the second proton (H2) of water moves to N2 on pyridine (PT2) at 76 fs (see atom numbering in Fig. 1). Finally, the tautomer (T) form is formed within 85 fs. After the tautomerization with water assistance is completed, PQ and water fragments dissociate.

The time evolution of the two bond-forming distances O1···H1 and N2···H2 and of the two bond-breaking distances N1–H1 and O1–H2 along the PT pathway of the ESDPT process averaged over the 12 trajectories are shown

in Fig. 4a. Along the dynamics, the two bond-forming distances decrease to covalent bond length, whereas the two bond-breaking distances increase. At 75 fs, the average values of N1···H1 and O1···H1 bond distances are equal (1.32 Å), which indicates the time for the PT1 process. The second PT occurs at 82 fs, since at this time the average bond distances of O1···H2 and N2···H2 are equal (1.33 Å). After 150 fs, the O1–H1 and the N2–H2 distances start to exhibit oscillations around their equilibrium values. The interval time of about 7 fs between first and second PT implies that the process is a concerted synchronous PT. The average times are summarized in TABLE 2.

The time evolution of the ground and excited state energies averaged over the same 12 trajectories exhibiting ESDPT is shown in Fig. 4b. The average S_1-S_0 energy gap gradually decreases during the first 120 fs. After that, the average energy gap is still close to 2 eV, indicating that the structure of PQ tends to be planar throughout the process [46]. This planarity of the PQ skeleton is confirmed by the average value of the torsion angle N1C1C2N2, which remains around 180º throughout the simulation time.

3.2.2 PQ(H_2O)$_2$ complex

From 50 trajectories computed for the PQ(H_2O)$_2$ complex, three exhibited excited-state triple proton transfer (ESTPT) (6% probability, TABLE 2). The PT process did not occur for 39 trajectories during the simulation time. Eight trajectories reached a region of internal conversion (crossing between the $\pi\pi^*$ and S_0 states). The details of the PT process can be seen in the selected trajectory pictured in Fig. 5. A normal (N) form is observed at time 0. The first proton (H1) leaves the pyrrole ring, moving towards the O1 atom (PT1) at 54 fs. The PT2 occurs at 66 fs when the second proton (H2) of water moves to the O2 acceptor of the second water, and, at the same time, the PT3 also takes place as the third proton (H3) moves from the second water to the N2 on pyridine. Completion of the ESTPT reaction is reached after 71 fs and followed by the separation of PQ and water fragments.

The time evolution of the three bond-breaking distances (N1–H1, O1–H2, and O2–H3) and of the three bond-forming distances (O1···H1, O2···H2, and N2···H3) averaged over the three trajectories exhibiting PT is shown in Fig. S4a of the Supplementary Material. Along the trajectories, the first PT occurs at 58 fs (N1···H1 and O1···H1 are equal to 1.28 Å) and the occurrences of the second PT (O1···H2 and O2···H2 equal to 1.32 Å) and of the third PT (O2···H3 and N2···H3 equal to 1.27 Å) are observed at 60 and 69 fs, respectively. This dynamic behavior is considered as a concerted synchronous PT process. Fig. S4b shows that the S_1–S_0 energy gap gradually decreases in the first 100 fs. After that, the energy gap is still around 2 eV, indicating that the PQ skeleton remains planar during the simulation time.

3.2.3 PQ(MeOH) complex

The ESDPT reaction occurred in 36 out of 50 trajectories (72% probability, TABLE 2), while no reaction was observed in one trajectory, and 13 trajectories reached the region of internal conversion. Snapshots for a selected trajectory are shown in Fig. 6. Beginning with the normal form (N) at time 0, the PT process is described in the following steps: First, the first proton (H1) moves from the pyrrole ring to the O1 atom (PT1) at 72 fs; then, the second proton (H2) of the methanol moves to the N2 in pyridine (PT2) at 79 fs. Finally, the tautomer (T) formation is complete with the assistance of methanol at 85 fs. After the tautomerization, the PQ and methanol fragments dissociate as in the case of the PQ(H_2O) complex.

The time evolution of the two bond-breaking distances (N1–H1 and O1–H2) and of the two bond-forming distances (O1···H1 and N2···H2) along the hydrogen-bonded network of the ESDPT process averaged over the 36 trajectories exhibiting ESDPT are depicted in Fig. S5a of the Supplementary Material. The intersection between the curves indicates that the first and second PT processes occur at 87 and 92 fs, respectively. This dynamic behavior indicates a concerted synchronous process. As in the previous cases, the S_1-S_0 energy gap gradually decreases in the first 100 fs. After that, the average energy difference is always slightly below 2.0 eV revealing that no approach to a conical intersection between the two states is reached within the simulation time.

3.2.4 PQ(MeOH)$_2$ complex

The ESTPT reaction occurred in 14 trajectories (28%, TABLE 2), while no reaction was observed in 26 trajectories within the simulation time. Ten trajectories reached a crossing region between the S_1 and S_0. The dynamic details of the PT process for a selected trajectory are illustrated in Fig. 7. Starting with the normal structure (N) at time 0, the complete process follows the following three steps: (1) the first proton (H1) moves from N1 to O1 (PT1) at 56 fs, (2) the second proton (H2) moves from the O1 of the first methanol to the O2 of the second methanol (PT2) at 60 fs, and (3) the third proton (H3) moves from O2 to N2 (PT3) starting at 63 fs until the methanol-assisted tautomerization (T) is completed. The complete ESTPT reaction is reached after 70 fs and followed by the separation of PQ and MeOH fragments.

The time evolutions of the three bond-breaking distances (N1–H1, O1–H2, and O2–H3) averaged over the 14 trajectories exhibiting ESTPT show steep increases, and simultaneously, the time evolutions of the bond-forming distances (O1···H1, O2···H2, and N2···H3) show steep decreases (Fig. S6a of the Supplementary Material). The first PT process occurs at 61 fs when the average O2···H3 and N2···H3 distances are equal (1.29 Å). The second proton transfers from the PQ molecule to the first methanol at 64 fs when the average N1···H1 and O1···H1 distances are both equal to

1.28 Å. The last PT occurs at 67 fs when the average O1···H2 and O2···H2 distances are equal (1.31 Å). Once more, the PT processes are concerted synchronous. The S_1–S_0 energy gap behaves like in the previous cases, with stabilization around 2 eV.

3.2.5 Comparative analysis

For all trajectory of complete ESPT of each complex, we computed the average energies of (S_0) and the first-excited ($\pi\pi^*$) states for the normal (N), intermediary (IS1, IS2, and IS3 (only complexes of PQ with two water and two methanol molecules)), and tautomer (T) structures along the reaction pathway. They are all listed in TABLE S3 in the Supplementary Material and figure 8. The results show that the average excited-state reaction path has barriers of 3 and 8 kcal.mol^{-1} for the PQ(H_2O) and PQ$(H_2O)_2$, while it is barrierless for PQ(MeOH) and PQ$(MeOH)_2$. The average excited-state barriers correlate well with the PT probability reported in TABLE 2. In particular, it supports why the probability of the PT reaction increases from 24% to 72% in the comparison between PQ(H_2O) and PQ(MeOH). The increase in the probability of PT between PQ$(H_2O)_2$ and PQ$(MeOH)_2$ from 6% to 28% is also rationalized. Moreover, the larger excited-state barrier for PQ$(H_2O)_{1\text{-}2}$ than for PQ$(MeOH)_{1\text{-}2}$ is in good agreement with calculated results [24] and LIF excitation spectrum [26].

For the PT time evolution, all complexes share a common pattern: after photoexcitation, it takes a relatively long time to initiate the PT process, between 58 and 87 fs (TABLE 2). However, as soon as the first PT is initiated, it triggers a fast sequence of proton transfers through the solvent bridge, until tautomerization is achieved within 92 fs. The delay between each PT is always under 9 fs, characterizing a concerted synchronous process. Independently of the solvent, the time for the first PT in PQ-solvent clusters is longer than that in HBT in water (10 fs), [14] but similar to those predicted for 7AI in methanol (57-71 fs) [9].

Our results clearly reveal that the initial PT time for PQ in water is slightly shorter than that in methanol about 10 fs. For n = 1, these times are 75 and 92 fs, whereas for n = 2, they are 58 and 69 fs. The delay times between each PT for PQ with one and two water molecules were found to be longer than those of PQ with one and two methanol molecules; however, they are still characteristics of concerted synchronous processes. The complete PT time decreases from 92 fs to 67 fs for PQ with water and from 92 fs to 67 fs for PQ with methanol when increasing the number of participating solvent molecules from one to two. This slight difference might be explained by the strength of hydrogen bond (HB) in PQ with more solvent molecules upon photoexcitation, which is stronger in the case of two solvent molecules compared to one solvent molecule (see values in TABLE 2) resulting in a faster complete PT time. In the

case of PQ(H_2O), its early starting of the first PT (compared to PQ(MeOH)) together with the planarity of its O1N1N2O2 dihedral angle contributes to a completion of the tautomerization process 10 fs faster than that in PQ(MeOH).

Our results show that the ESmultiPT process of PQ with water and methanol is cluster-size selective. The stoichiometry of 1:1 complexes exhibits higher efficiency than that of 1:2 complexes for both solvents, as revealed by the PT probabilities. In particular, one single methanol molecule seems to facilitate the tautomerization reaction most effectively among all investigated complexes.

4. Conclusions

The ground-state structures of PQ$(H_2O)_{n=1,2}$ and PQ$(MeOH)_{n=1,2}$ complexes at the RI-ADC(2)/SVP level were investigated. It was found that intermolecular hydrogen bonds of PQ with water and methanol become stronger when the number of solvent molecules increases. Excited-state dynamics simulations were performed to reveal details of the excited-state PT pathways for all reactions within PQ$(H_2O)_{n=1,2}$ and PQ$(MeOH)_{n=1,2}$ complexes. The excited-state proton transfer reactions are ultrafast processes depending on the cluster size. Phototautomerization of all complexes occurs in less than 92 fs. Moreover, the ESPT process was found to have a concerted synchronous mechanism for all complexes, with delay times between proton transfers always under 9 fs. Our investigations also show that the intermolecular ESPT in the first excited state occurs along a pathway with $\pi\pi^*$ character, located within the π system of PQ, regardless of the solvent partner. No crossing between $\pi\pi^*$ and $\pi\sigma^*$ states is observed. Thus, these transfer processes are characterized as PT and not as HT.

Acknowledgement – The authors wish to thank the Thailand Research Fund (TRF) (MRG5480294) for financial support. This work is also partially supported by TRF (RTA5380010). The computer facility at the Department of Chemistry, Faculty of Science, Chiang Mai University, Chiang Mai, Thailand is also acknowledged.

Electronic Supplementary Material: Cartesian coordinates of ground-state optimized structures. Potential-energy diagrams for selected trajectories. Time evolution of geometrical and energetic variables.

References

1. Arnaut LG, Formosinho SJ (1993) J Photochem Photobiol A 75:1-20.

2. Formosinho SJ, Arnaut LG (1993) J Photochem Photobiol A 75:21-48.

3. Han K-L, Zhao G-J (2011) Hydrogen Bonding and Transfer in the Excited State, Volume II. vol Copyright (C) 2011 American Chemical Society (ACS). All Rights Reserved. John Wiley & Sons Ltd.,

4. Zhao G-J, Han K-L (2012) Acc Chem Res 45:404-413.

5. Gordon MS (1996) J Phys Chem 100:3974-3979.

6. Mente S, Maroncelli M (1998) J Phys Chem A 102:3860-3876.

7. Waluk J (2003) Acc Chem Res 36:832-838.

8. Reyman D, Díaz-Oliva C (2011) Excited-State Double Hydrogen Bonding Induced by Charge Transfer in Isomeric Bifunctional Azaaromatic Compounds. Hydrogen Bonding and Transfer in the Excited State, Volume I & II:661-709

9. Daengngern R, Kungwan N, Wolschann P, Aquino AJA, Lischka H, Barbatti M (2011) J Phys Chem A 115:14129-14136.

10. Sakota K, Jouvet C, Dedonder C, Fujii M, Sekiya H (2010) J Phys Chem A 114:11161-11166.

11. Filarowski A, Koll A, Hansen PE, Kluba M (2008) J Phys Chem A 112:3478-3485.

12. Filarowski A, Majerz I (2008) J Phys Chem A 112:3119-3126.

13. Jezierska-Mazzarello A, Vuilleumier R, Panek JJ, Ciccotti G (2010) J Phys Chem B 114:242-253.

14. Kungwan N, Plasser F, Aquino AJA, Barbatti M, Wolschann P, Lischka H (2012) Phys Chem Chem Phys 14:9016-9025.

15. Hara A, Sakota K, Nakagaki M, Sekiya H (2005) Chem Phys Lett 407:30-34.

16. Sakota K, Komoto Y, Nakagaki M, Ishikawa W, Sekiya H (2007) Chem Phys Lett 435:1-4.

17. Sakota K, Inoue N, Komoto Y, Sekiya H (2007) J Phys Chem A 111:4596-4603.

18. Taylor CA, El-Bayoumi MA, Kasha M (1969) Proc Natl Acad Sci USA 63:253-260.

19. Ilich P (1995) J Mol Struct 354:37-47.

20. Kina D, Nakayama A, Noro T, Taketsugu T, Gordon MS (2008) J Phys Chem A 112:9675-9683.

21. Fernández-Ramos A, Martínez-Núñez E, Vázquez SA, Ríos MA, Estévez CM, Merchán M, Serrano-Andrés L (2007) J Phys Chem A 111:5907-5912.

22. Guglielmi M, Tavernelli I, Rothlisberger U (2009) Phys Chem Chem Phys 11:4549-4555

23. Park SY, Jang DJ (2009) J Am Chem Soc 132:297-302.

24. Kyrychenko A, Waluk J (2006) J Phys Chem A 110:11958-11967.

25. Nosenko Y, Kunitski M, Thummel RP, Kyrychenko A, Herbich J, Waluk J, Riehn C, Brutschy B (2006) J Am Chem Soc 128:10000-10001.

26. Nosenko Y, Kyrychenko A, Thummel RP, Waluk J, Brutschy B, Herbich J (2007) Phys Chem Chem Phys 9:3276-3285.

27. Nosenko Y, Kunitski M, Riehn C, Thummel RP, Kyrychenko A, Herbich J, Waluk J, Brutschy B (2008) J Phys Chem A 112:1150-1156.

28. Gorski A, Gawinkowski S, Herbich J, Krauss O, Brutschy B, Thummel RP, Waluk J (2012) The Journal of Physical Chemistry A 116:11973-11986.
29. Wiosna G, Petkova I, Mudadu MS, Thummel RP, Waluk J (2004) Chem Phys Lett 400:379-383.
30. Kyrychenko A, Herbich J, Izydorzak M, Wu F, Thummel RP, Waluk J (1999) J Am Chem Soc 121:11179-11188.
31. Kyrychenko A, Herbich J, Wu F, Thummel RP, Waluk J (2000) J Am Chem Soc 122:2818-2827.
32. Ferlin MG, Chiarelotto G, Baccichetti F, Carlassare F, Toniolo L, Bordin F (1992) Farmaco 47:1513-1528.
33. Herbich J, Dobkowski J, Thummel RP, Hegde V, Waluk J (1997) J Phys Chem A 101:5839-5845.
34. Kyrychenko A, Stepanenko Y, Waluk J (2000) J Phys Chem A 104:9542-9555.
35. Hättig C (2003) J Chem Phys 118:7751-7761.
36. Hättig C (2005) Adv Quantum Chem 50:37-60.
37. Schäfer A, Horn H, Ahlrichs R (1992) J Chem Phys 97:2571-2577.
38. Ahlrichs R, Bär M, Häser M, Horn H, Kölmel C (1989) Chem Phys Lett 162:165-169.
39. Barbatti M, Aquino AJA, Lischka H (2010) Phys Chem Chem Phys 12:4959-4967.
40. Barbatti M, Granucci G, Ruckenbauer M, Plasser F, Pittner J, Persico M, Lischka H (2011) Newton-X: a package for Newtonian dynamics close to the crossing seam, version 12, wwwnewtonxorg.
41. Barbatti M, Granucci G, Persico M, Ruckenbauer M, Vazdar M, Eckert-Maksic M, Lischka H (2007) J Photochem Photobiol, A 190:228-240.
42. Barbatti M, Aquino AJA, Lischka H, Schriever C, Lochbrunner S, Riedle E (2009) Phys Chem Chem Phys 11:1406-1415.
43. Dewar MJS (1984) J Am Chem Soc 106:209-219.
44. Al-Lawatia N, Husband J, Steinbrecher T, Abou-Zied OK (2011) J Phys Chem A 115:4195-4201.
45. Tanner C, Manca C, Leutwyler S (2003) Science (Washington, DC, U S) 302:1736-1739.
46. Barbatti M, Aquino AJA, Lischka H, Schriever C, Lochbrunner S, Riedle E (2009) Phys Chem Chem Phys 11:1406-1415.

TABLE

TABLE 1: Summary of the ground-state structures computed at RI-ADC(2)/SVP level. Distances in Å, dihedral angles (ø N1C1C2N2 and ∠O1N1N2O2) in degrees.

	Complex			
	PQ(H_2O)	**PQ(H_2O)$_2$**	**PQ(MeOH)**	**PQ(MeOH)$_2$**
R_1	1.814	1.786	1.794 (1.872) [a]	1.743 (1.765)
R_2	1.866	1.794	1.820 (1.835)	1.755 (1.786)
R_3		1.750		1.720 (1.762)
N1–O1	2.804	2.807	2.776	2.775
O[b]–N2	2.822	2.775	2.778	2.740
O1–O2		2.694		2.656
ø	5.2	2.9	-4.5	2.4
∠		-20.3		-33.4

[a] RI-MP2 level [26] for PQ with methanol in parentheses, [b] O1 for one water or methanol, O2 for two water or methanol molecules

TABLE 2: Summary of the excited-state dynamics at RI-ADC(2)/SVP-SV(P) level of $PQ(H_2O)_{n=1,2}$ and $PQ(MeOH)_{n=1,2}$ complexes. Average distances (in Å) for PT time in parentheses.

Complex	Number of trajectories			ESPT Probability	Time (fs)		
	ESPT ($\pi\pi^*$)	IC ($\pi\pi^*/S_0$)	NT		PT1	PT2	PT3
$PQ(H_2O)$	12	7	31	0.24	75 (1.32)	82 (1.33)	
$PQ(H_2O)_2$	3	8	39	0.06	58 (1.28)	60 (1.32)	69 (1.27)
PQ(MeOH)	36	13	1	0.72	87 (1.32)	92 (1.32)	
$PQ(MeOH)_2$	14	10	26	0.28	61 (1.29)	64 (1.28)	67 (1.31)

Figures

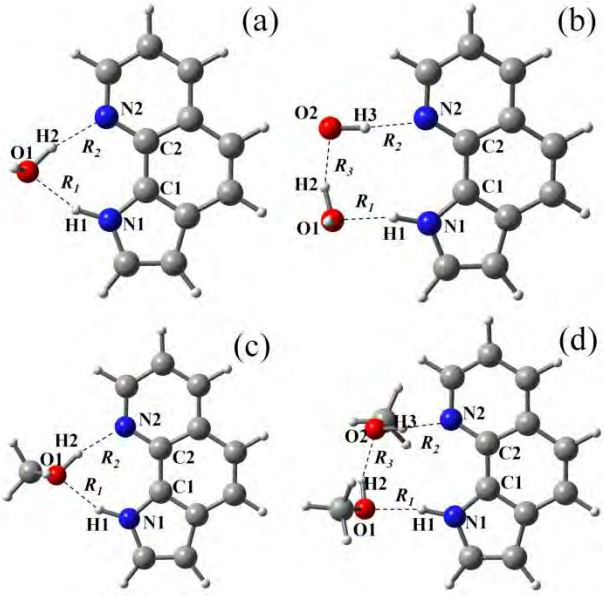

Fig 1

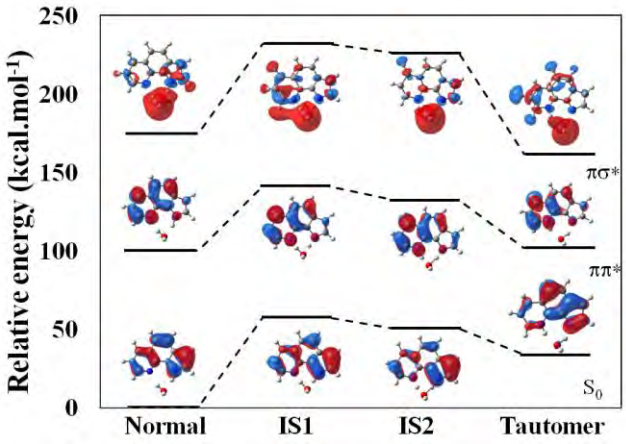
250
200
150
100
50
0
Relative energy (kcal.mol-1)
πσ*
ππ*
S0
Normal
IS1
IS2
Tautomer

Fig 2

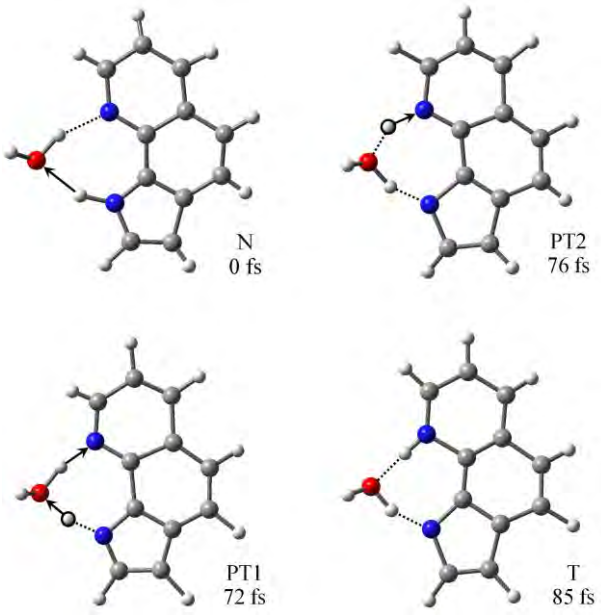

Fig 3

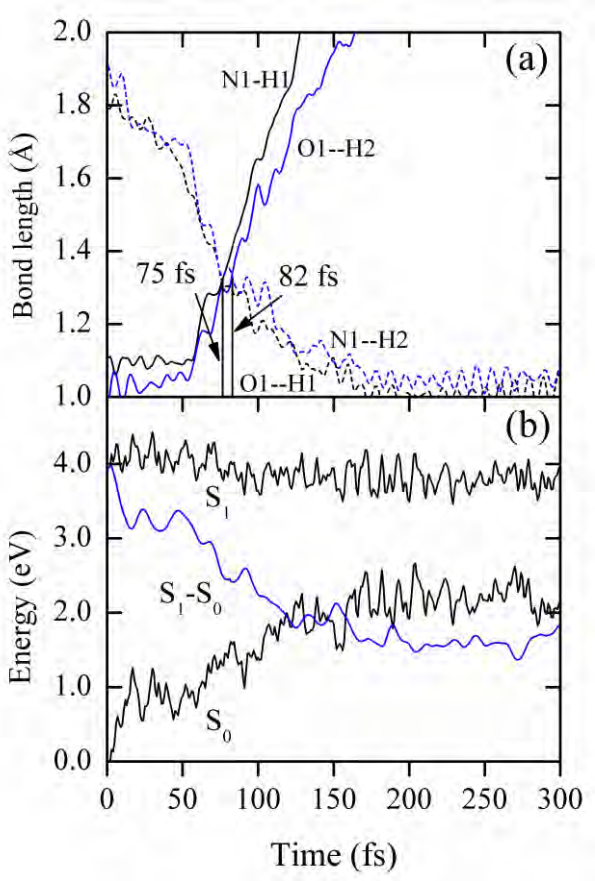
(a)
N1-H1
O1--H2
75 fs
82 fs
N1--H2
O1--H1
Bond length (Å)
2.0
1.8
1.6
1.4
1.2
1.0
(b)
S1
S1-S0
S0
Energy (eV)
4.0
3.0
2.0
1.0
0.0
0
50
100
150
200
250
300
Time (fs)

Fig 4

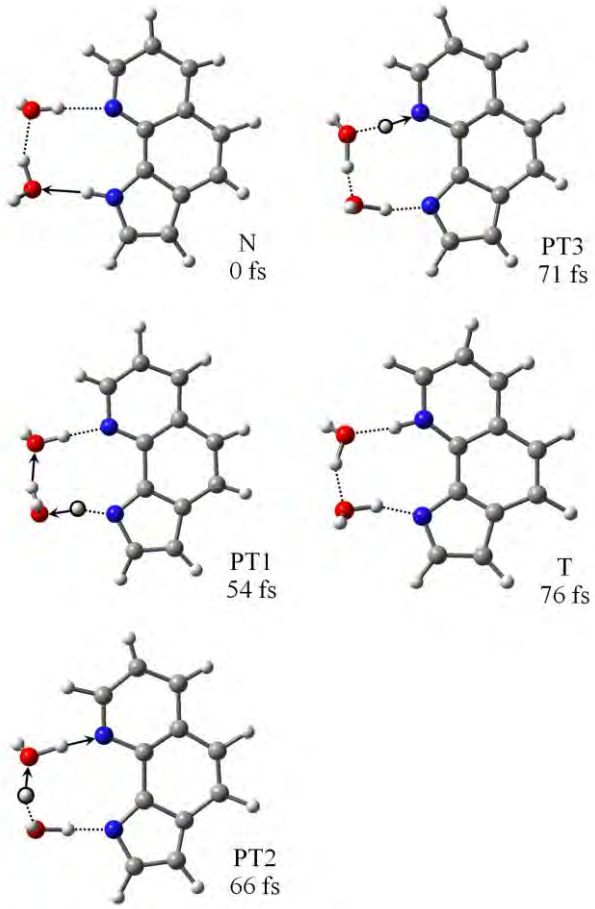

Fig 5

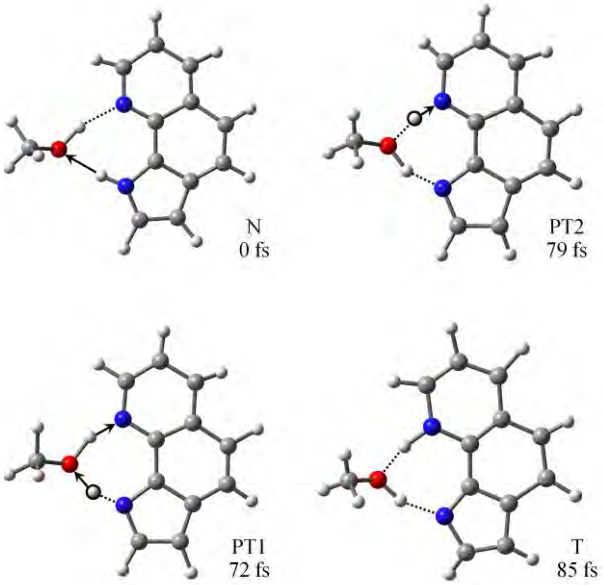

Fig 6

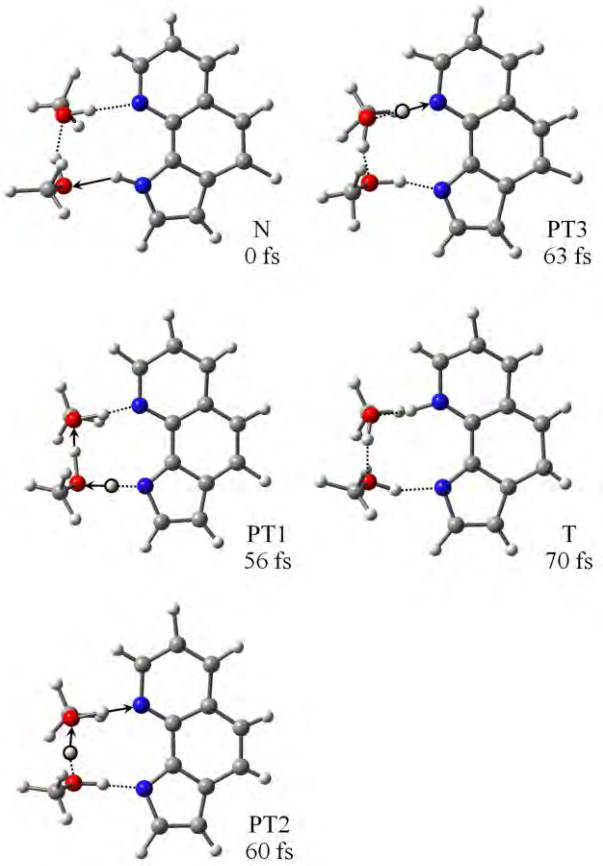

Fig 7

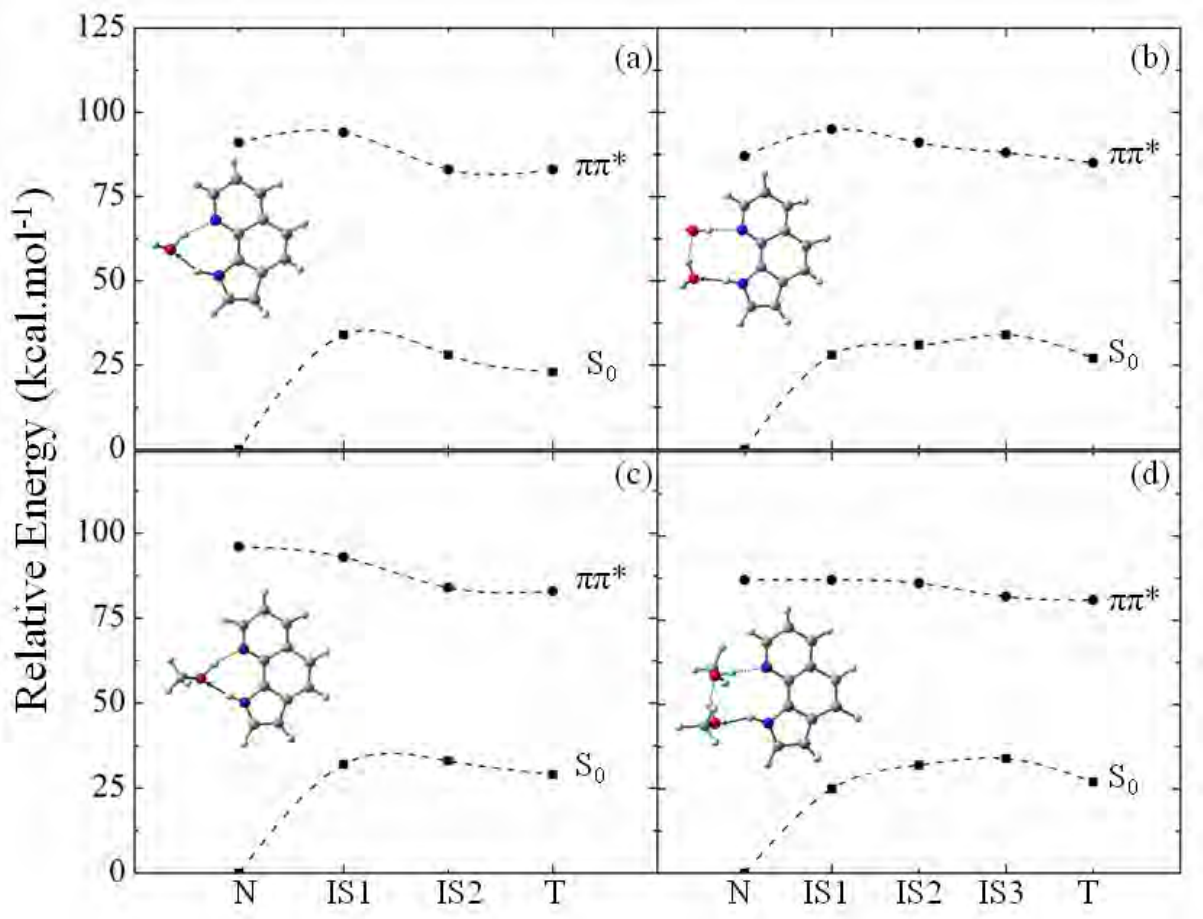
Relative Energy (kcal.mol-1)
125
100
75
50
25
0
(a)
(b)
(c)
(d)
ππ*
S0
N
IS1
IS2
IS3
T

Fig 8

Graphical Abstract

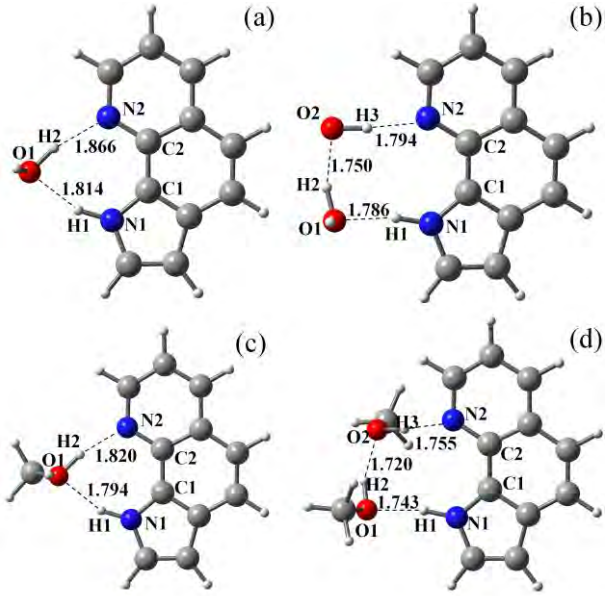

Figure1
Click here to download high resolution image

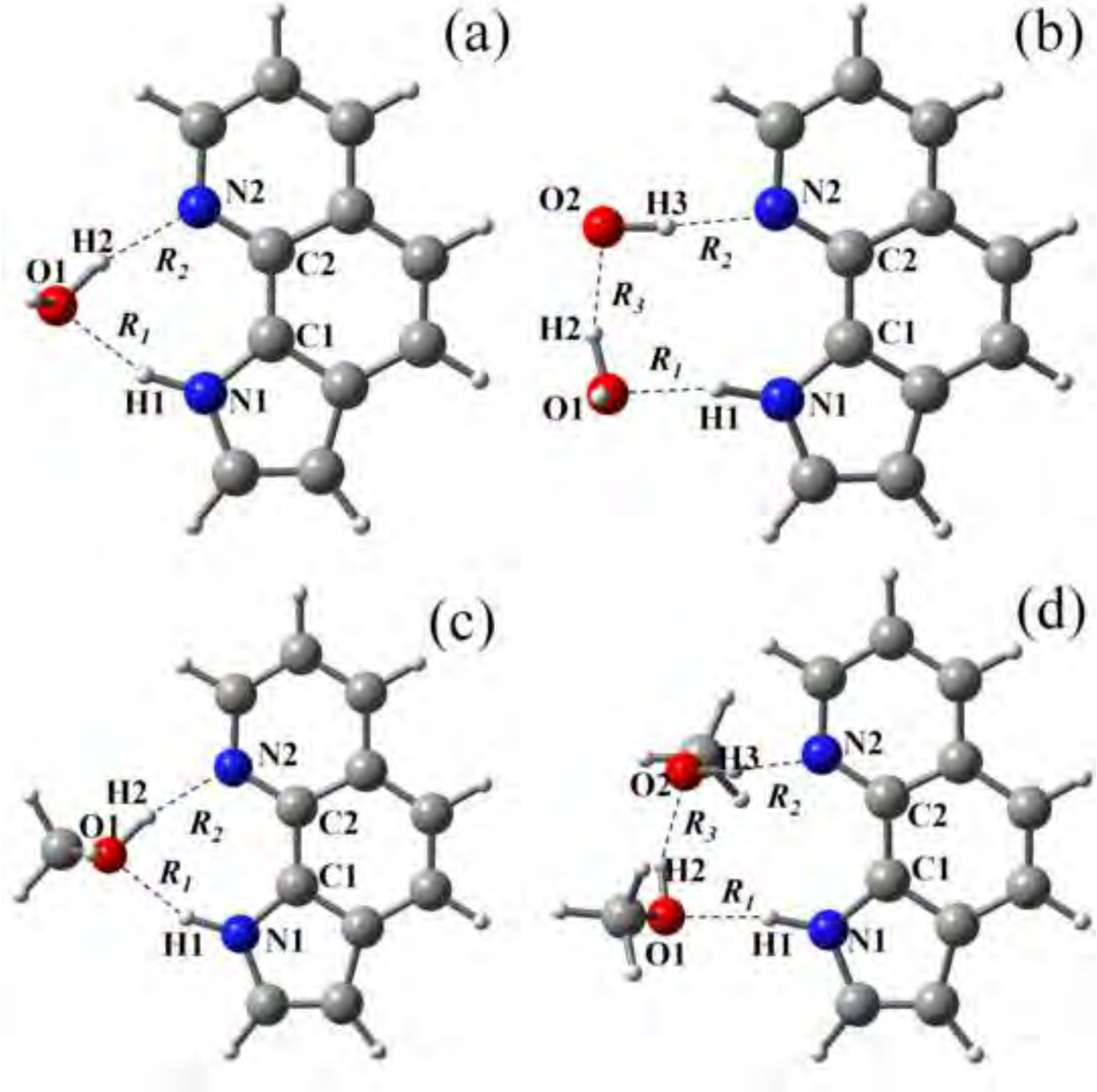

Figure2
Click here to download high resolution image

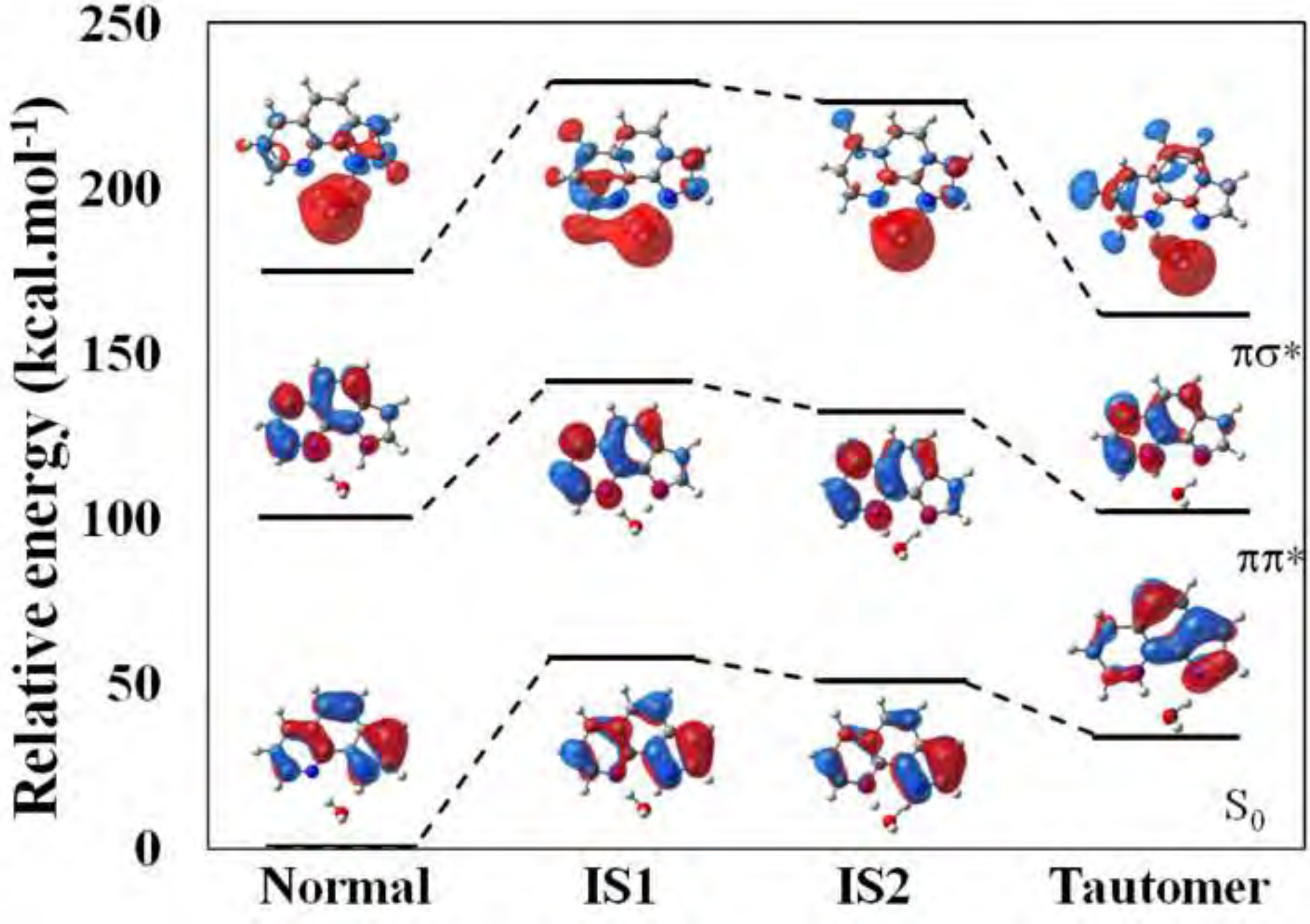

Figure3
Click here to download high resolution image

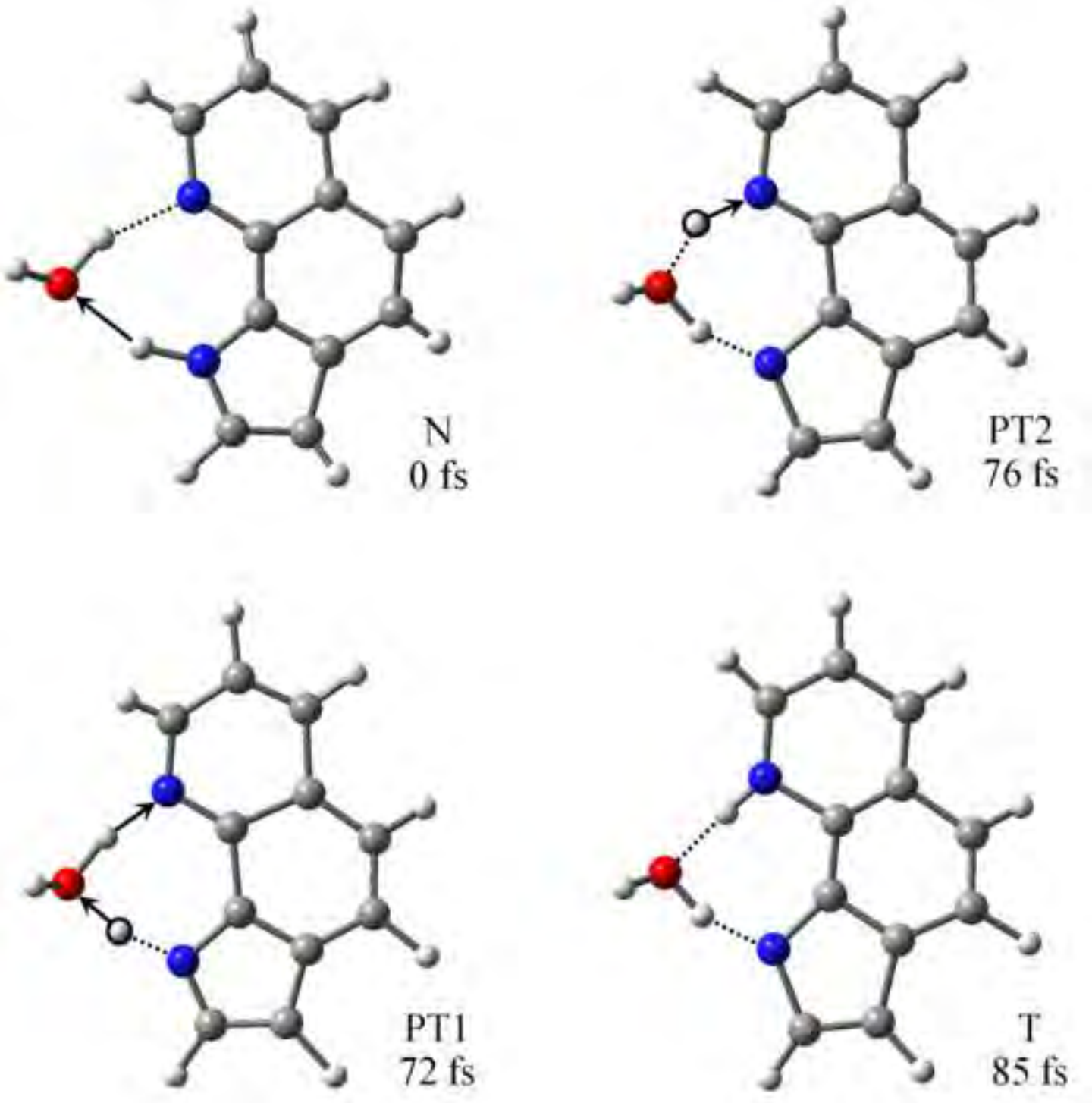

Figure4
Click here to download high resolution image

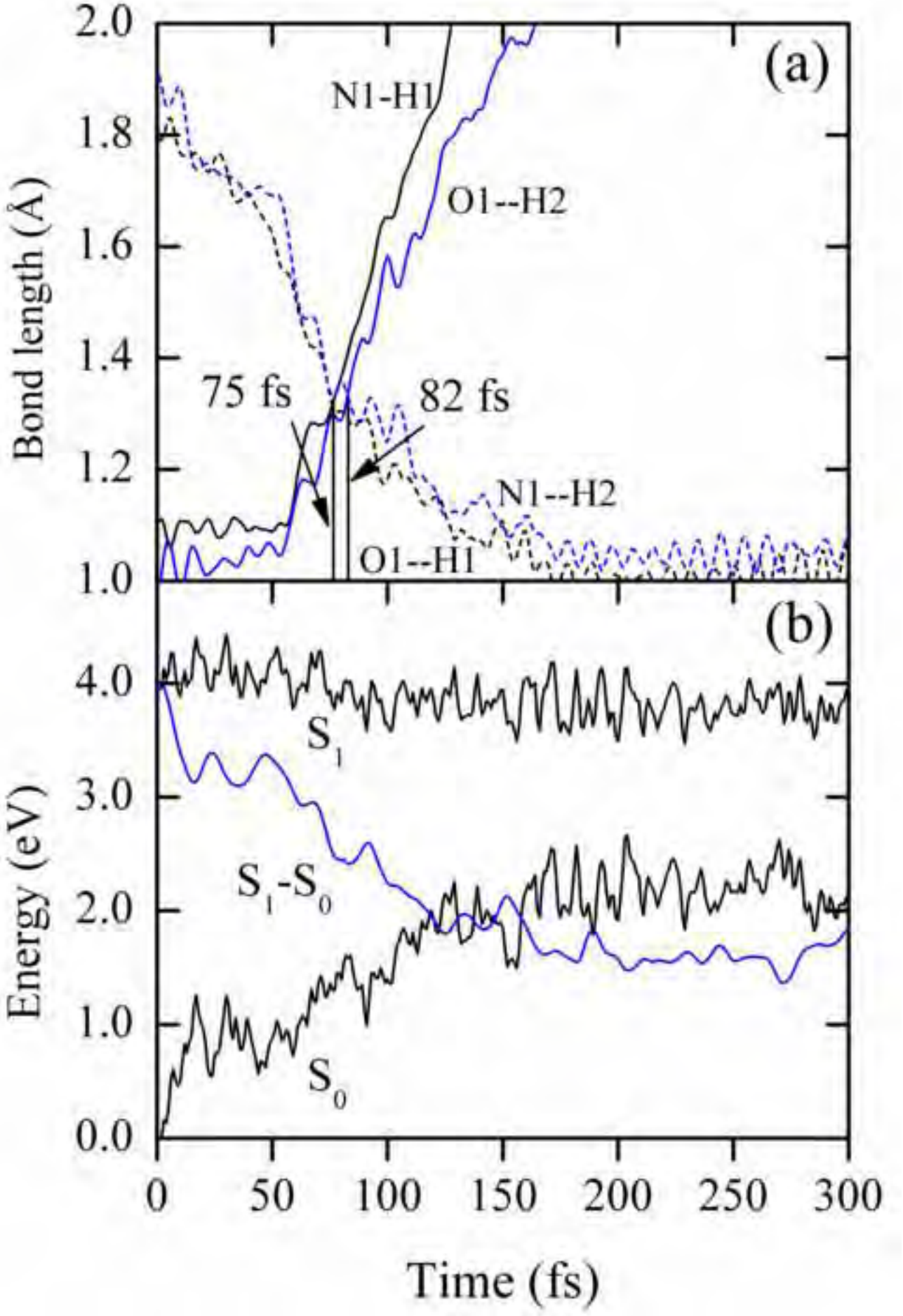

Figure5
Click here to download high resolution image

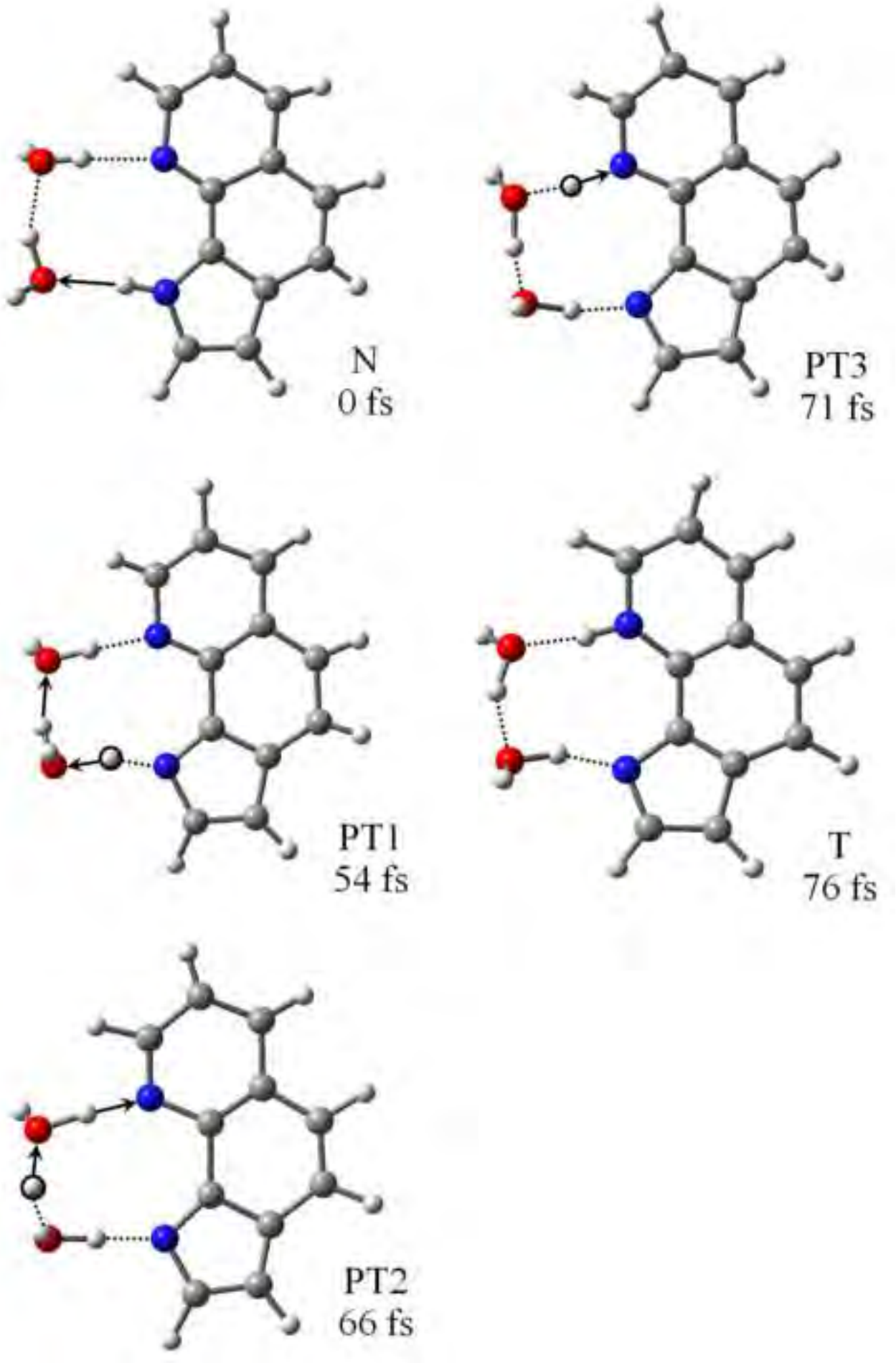

Figure6
Click here to download high resolution image

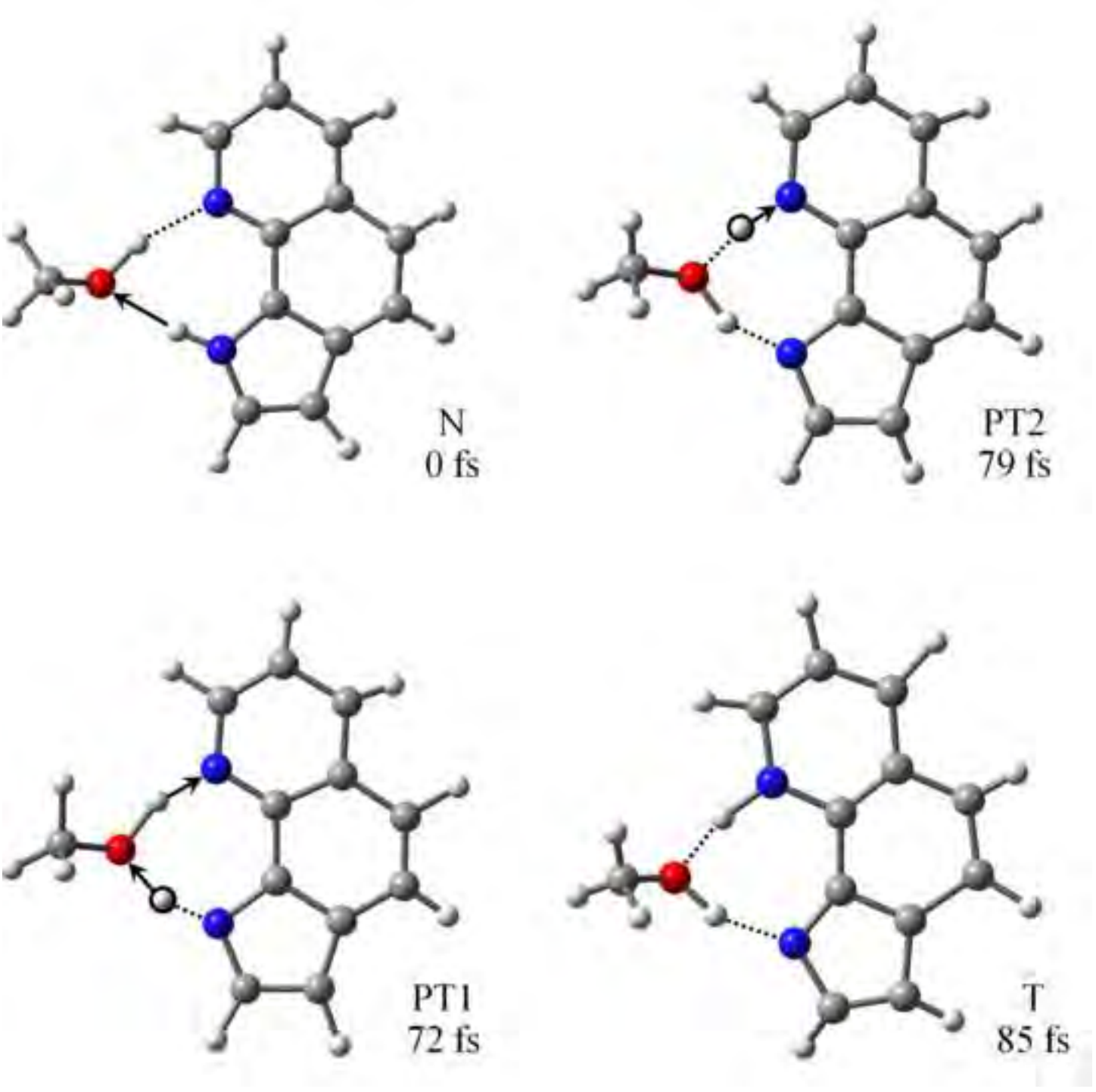

Figure7
Click here to download high resolution image

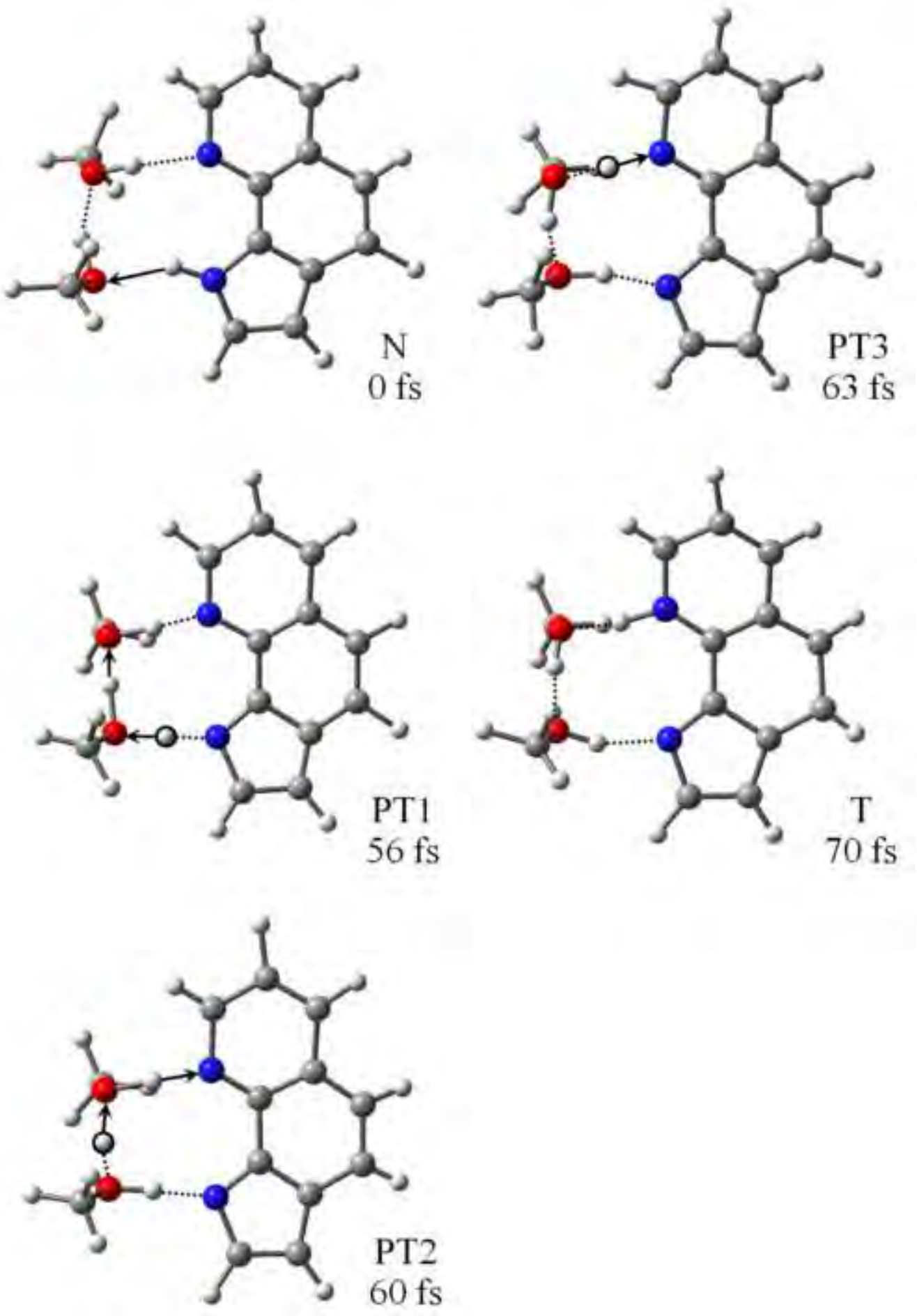

Figure8
Click here to download high resolution image

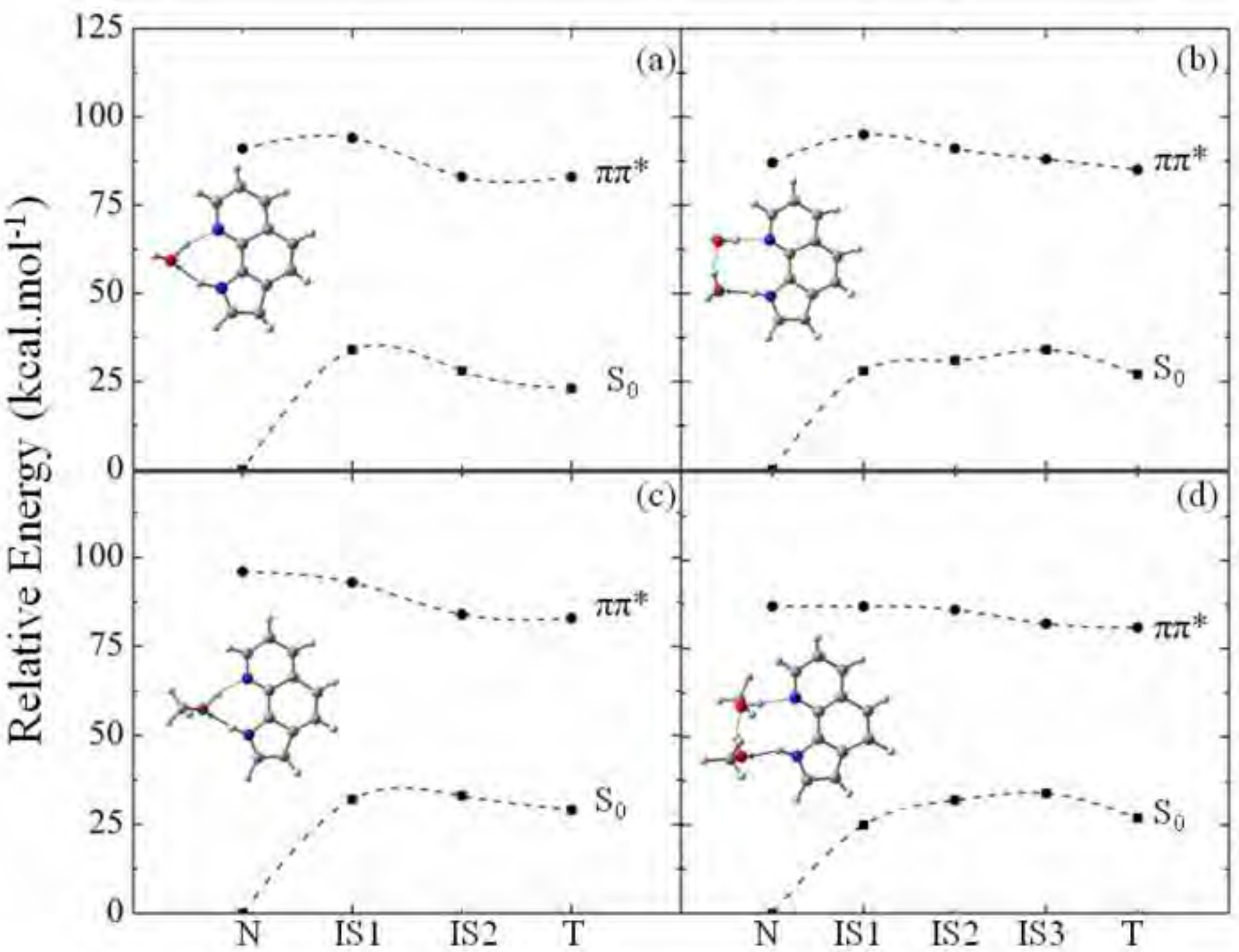

Graphical abstract

Click here to download high resolution image

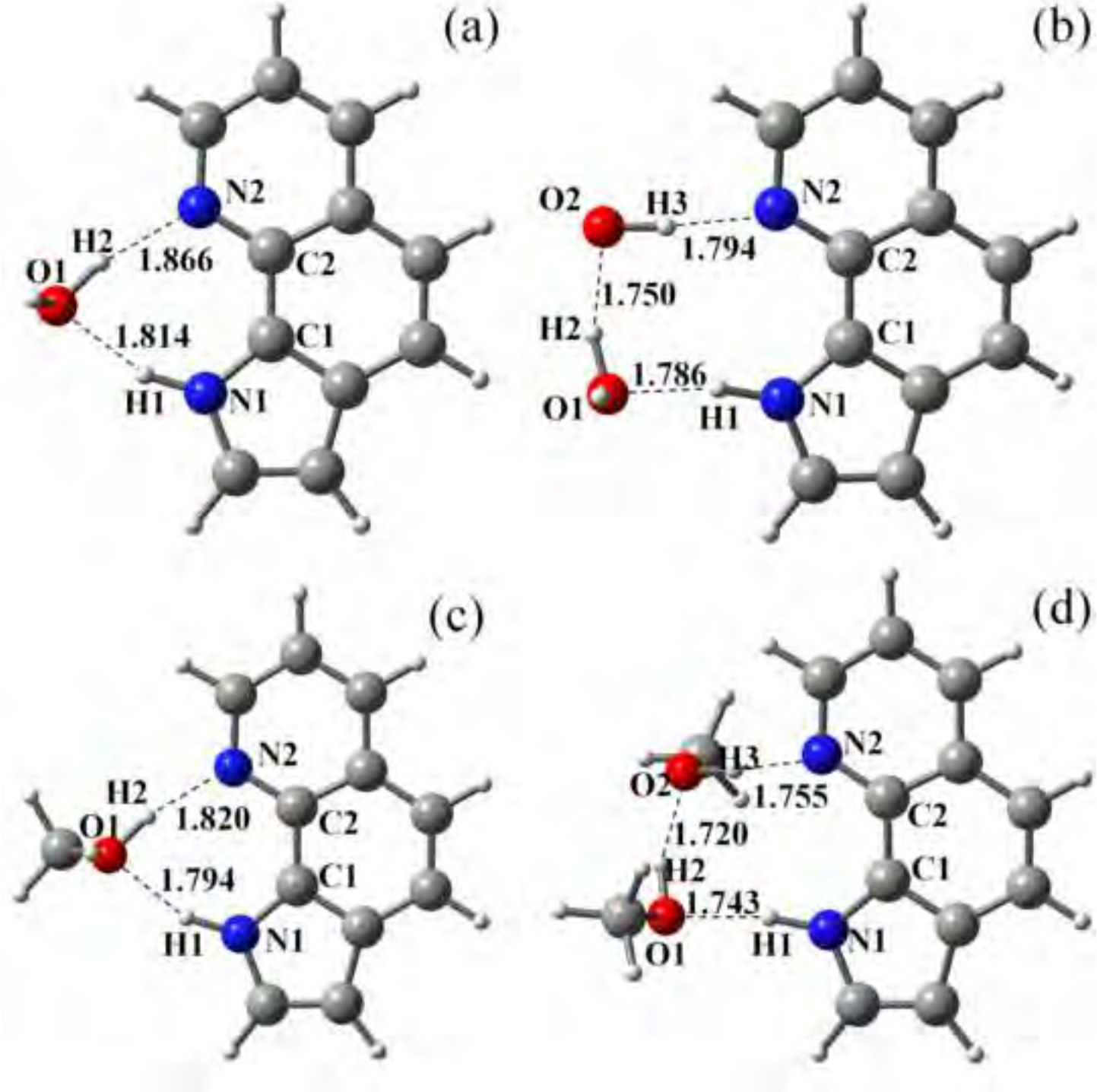

Figure Captions

Figure 1. The ground-state optimized structures of $PQ(H_2O)_n$ and $PQ(MeOH)_n$ (n = 1,2) complexes at the RI-ADC(2)/SVP level. Atom numbering for intermolecular hydrogen bonds to water and methanol molecules (a) $PQ(H_2O)$ (b) $PQ(H_2O)_2$ (c) PQ(MeOH) and (d) $PQ(MeOH)_2$. Intermolecular hydrogen-bonded interactions are presented by dashed lines.

Figure 2. Potential-energy diagram of the ground state (S_0) and excited states ($\pi\pi^*$, $\pi\sigma^*$) of a selected trajectory for the $PQ(H_2O)$ complex.

Figure 3. Snapshots from a selected trajectory of the $PQ(H_2O)$ dynamics showing the time evolution of the ESDPT reaction through the hydrogen-bonded network within 85 fs. Normal (N), Proton transfer (PT), and Tautomer (T).

Figure 4. Average properties over the 12 trajectories of the $PQ(H_2O)$ complex exhibiting ESDPT, as a function of time: (a) Average lengths of broken and new bonds; (b) Average relative energies of the excited state (S_1), ground state (S_0), and the S_1-S_0 energy gap.

Figure 5. Snapshots from a selected trajectory of the $PQ(H_2O)_2$ complex showing the time evolution of the ESTPT reaction through the hydrogen-bonded network, occurring within 76 fs.

Figure 6. Snapshots from a selected trajectory of the PQ(MeOH) dynamics showing the time evolution of the ESDPT reaction through the hydrogen-bonded network, occurring within 85 fs.

Figure 7. Snapshots from a selected trajectory of the $PQ(MeOH)_2$ dynamics showing the time evolution of the ESTPT reaction through the hydrogen-bonded network, occurring within 70 fs.

Figure 8. Average Relative energies ($kcal.mol^{-1}$) of the ground (S_0) and the excited states ($\pi\pi^*$) of (a) $PQ(H_2O)$, (b) $PQ(H_2O)_2$, (c) PQ(MeOH), and (d) $PQ(MeOH)_2$ complexes.

TABLE

TABLE 1: Summary of the Ground-State Structures Computed at RI-ADC(2)/SVP Level. Distances in Å, Dihedral Angles (ø N1C1C2N2 and ∠O1N1N2O2) in Degrees.

	Complex			
	PQ(H_2O)	**PQ(H_2O)$_2$**	**PQ(MeOH)**	**PQ(MeOH)$_2$**
R_1	1.814	1.786	1.794	1.743
			(1.872) [a]	(1.765)
R_2	1.866	1.794	1.820	1.755
			(1.835)	(1.786)
R_3		1.750		1.720
				(1.762)
N1–O1	2.804	2.807	2.776	2.775
O[b]–N2	2.822	2.775	2.778	2.740
O1–O2		2.694		2.656
ø	5.2	2.9	-4.5	2.4
∠		-20.3		-33.4

[a] RI-MP2 level [26] for PQ with methanol in parentheses, [b] O1 for one water or methanol, O2 for two water or methanol molecules

TABLE 2: Summary of the Excited-State Dynamics at RI-ADC(2)/SVP-SV(P) Level of $PQ(H_2O)_{n=1,2}$ and $PQ(MeOH)_{n=1,2}$ Complexes. Average distances (in Å) for PT Time in Parentheses.

Complex	Number of trajectories			ESPT Probability	Time (fs)		
	ESPT ($\pi\pi^*$)	IC ($\pi\pi^*/S_0$)	NT		PT1	PT2	PT3
$PQ(H_2O)$	12	7	31	0.24	75 (1.32)	82 (1.33)	
$PQ(H_2O)_2$	3	8	39	0.06	58 (1.28)	60 (1.32)	69 (1.27)
PQ(MeOH)	36	13	1	0.72	87 (1.32)	92 (1.32)	
$PQ(MeOH)_2$	14	10	26	0.28	61 (1.29)	64 (1.28)	67 (1.31)